Artificial Entanglements in Polymer Chains

Development and Validation of a Multi Chain Slip-Spring Model in Dissipative Particle Dynamics Simulations

TECHNISCHE UNIVERSITÄT DARMSTADT

Vom Fachbereich Chemie

der Technischen Universität Darmstadt

zur Erlangung des akademischen Grades eines

Doktor-Ingenieurs (Dr.-Ing.)

genehmigte

Dissertation

vorgelegt von

Dipl.-Ing. Michael Langeloth

aus Frankfurt am Main.

Referent: Prof. Dr. Müller Plathe

Korreferent: Prof. Dr. van der Vegt,

Prof. Dr. Everaers

Tag der Einreichung: 24. April 2015

Tag der mündlichen Prüfung: 08. Juni 2015

Darmstadt 2015

D17

Zusammenfassung:

Wir stellen eine neue Technik vor, mit deren Hilfe Verschlaufungen, sogenannte „Entanglements“, in stark vergröberten Polymerketten in Molekular-Simulationen zu behandeln. Diese Verschlaufungen sind sehr wichtig für das dynamische Verhalten der Ketten und bestimmen die Rheologie des Materials. Molekular-Simulationen nutzen oftmals eine vergröberte Darstellung der Moleküle um Rechenzeit zu sparen. Dies ist besonders wichtig bei der Simulation von Polymeren aufgrund der weiten Zeit und Längen Skalen. Hierbei wird die Kette nicht durch ihre einzelnen Atome, sondern durch wenige Wiederholungseinheiten dargestellt. Diese Kugeln können mehrere Atome, Monomere oder sogar ganze Kettensegmente repräsentieren könne. Die resultierenden nichtbindenden Wechselwirkungen zwischen den Kugeln nehmen mit der Vergröberung ab, um die Kettenstatistik beizubehalten. Bei starker Vergröberung reichen die nichtbindenden Wechselwirkungen nicht aus um die Ketten auseinander zu halten. Die Ketten können sich dann einfach kreuzen. Daraus folgt, dass diese sich nicht mit ihren benachbarten Ketten verschlaufen können. Die Abwesenheit der Verschlaufungen führt zu einer beschleunigten Polymerdynamik. Wichtige dynamische Eigenschaften wie Diffusion oder Viskosität, werden im Vergleich zu verschlauften Polymeren deutlich überschätzt. Das viskoelastische Verhalten, eine Schlüsseleigenschaft die Polymere im Vergleich zu anderen Materialen auszeichnet, ist ohne Verschlaufungen nicht mehr vorhanden. Die vorgestellte Methode fügt künstliche Bindungen in das System ein um den Verlust an Verschlaufungen zu kompensieren. Diese Bindungen aehneln dabei den Verbindungen in einem Netzwerk. Allerdings, ist im Unterschied zum Netzwerk ihre Position nicht fest. Die Bindungen können sich entlang der Kette bewegen und können am Kettenende gebildet und zerstört werden. Aus dieser Bewegung entstamm auch der Name „slip-springs“ fuer die Bindungen.
Durch diese „slip-springs“ wird die Kettendynamik so beeinflusst, dass sie der von Ketten mit Verschlaufungen gleicht. Die statischen Eigenschaften der Ketten bleiben dabei unberührt. Die hier vorgestellte Methode unterscheidet sich von vielen bereits existierenden „slip-spring“ oder „slip-link“ Methoden durch die Kombination mit „Dissipative Particle Dynamics“. Einer Simulationsmethode, die über ein besonderes Thermostat verfügt, welches Impulserhaltung lokal gewährleistet und sich somit für die Berechnung von

hydrodynamischen Wechselwirkungen anbietet. Dies ist eine Vorraussetzung für die Behandlung von Polymeren in Lösung. Untersucht wurden mit unserer „slip-spring“ Methode die dynamischen Eigenschaften linearer Ketten in mono- und bidispersen Schmelzen, sowie in Polymer Lösungen. Das Verhalten ist konsistent mit den theoretischen Erwartungen oder experimentellen Beobachtungen. Das Modell kann somit Rouse bzw. Zimm Verhalten für unverschlaufte Ketten, als auch das Reptations Verhalten für verschlaufte Ketten, einschließlich des Übergangs beider Regime darstellen. Unser Model zeichnet sich dadurch aus, dass sich die Dynamik in allen Regimen a posteriori einstellt und somit keine zusätzlichen Parameter benötigt werden. Im Vergleich zu konventionellen „Molecular Dynamics“ Simulationen, bei denen die Ketten durch die Wechselwirkungen mit harten Kernen davon abgehalten werden sich gegenseitig zu kreuzen, hat sich gezeigt, dass unsere Methode zwei Größenordnungen schneller ist. Die Methode bietet sich somit für vielfältige Anwendungen mit langen, verschlauften Polymeren an.

Abstract:

We introduce a novel technique that facilitates entangled dynamics of coarse-grained polymer chains in Molecular simulations. Entanglements are very important for the dynamic properties of the chains and affect the rheology of the material. Molecular simulations often use a coarse-grained description of the molecules in order to reduce the time for computation. This is important especially for polymer simulations because of the enormous time and length scales of interest. Hence, a chain is not modeled by all its single atoms, but by only a few repeating units. These beads may represent several atoms, monomers or even entire segments of the chain. However, the nonbonded potential between two beads becomes softer with the level of coarse-graining in order to maintain the static properties of the chain. For highly coarse-grained models, the nonbonded potentials may not be strong enough to keep two chains apart. Then, the chains can simply pass through each other. As a consequence, they cannot entangle with their neighboring chains anymore. The absence of entanglements accelerates the chain dynamics. Important dynamic properties like diffusion or viscosity are overestimated compared to entangled chains. The viscoelastic behavior, a key property that distinguishes polymers from other types of material, is also gone with the entanglements.

The present method inserts artificial bonds into the system in order to compensate for the loss of the entanglements. These bonds act like cross-links in a polymeric network. However, the position of the artificial bonds is not fixed, in contrast to cross-links. They may move along the chain in discrete steps and can be created or terminated at the chain ends. Hence, they are called “slip-springs”. The slip-springs affect the chain dynamics in a way such that it becomes consistent with entangled dynamics. The static properties of the chains remain unaffected by the insertion and motion of the slip-springs. In contrast to other existing slip-link or slip-spring models, the present model employs dissipative particle dynamics. This simulation technique uses a special thermostat that ensures that momentum is locally conserved, which is a prerequisite for hydrodynamic interactions. The applicability of the “slip-spring” method has been verified for monodisperse and bidisperse melts as well as polymer solutions. The dynamic behavior is consistent with theoretical predictions or experimental observations. Hence, the model can describe Rouse, or Zimm behavior for unentangled chains, as well as reptation

dynamics for entangled chains, including the transition between these regimes. The present model distinguishes itself from other slip-link or slip-spring approaches by the fact that the dynamics in all regimes is obtained a posteriori without the need of additional parameters. The present technique is two orders of magnitude faster than conventional Molecular Dynamics simulations that retain the chain uncrossability by excluded volume interactions of the beads. Therefore, the method is well-suited for a variety of applications with long, entangled polymer chains.

Dies ist eine kumulative Dissertation, bestehend aus den folgenden 3 Veröffentlichungen:

M. Langeloth, Y. Masubuchi, M.C. Böhm, and F. Müller-Plathe, *Recovering the reptation dynamics of polymer melts in dissipative particle dynamics simulations via slip-springs*, J. Chem. Phys. **138**, 104907 (2013).

M. Langeloth, Y. Masubuchi, M.C. Böhm, and F. Müller-Plathe, *Reptation and constraint release dynamics in bidisperse polymer melts*, J. Chem. Phys. **141**, 194904 (2014).

M. Langeloth, Y. Masubuchi, M.C. Böhm, and F. Müller-Plathe, *Dissipative particle dynamics simulation with slip-springs predicts the rheology of entangled polymers in solution*, Macromolecules, submitted, (2015).

Darin nicht enthalten, aber im gleichen Zeitraum entstanden, ist:

M. Langeloth, T. Sugii, M.C. Böhm, and F. Müller-Plathe, *Formation of the interphase of a cured epoxy resin near a metal surface: Coarse-grained reactive molecular dynamics simulations*, Soft Mater. **12**, 71-79 (2014).

Content

1. Introduction:

The main objective of this study has been the development and validation of a novel algorithm that facilitates mesoscopic simulations of entangled polymer chains. The idea has been derived from a previous project in this group which was about polymerization reactions in Molecular Dynamics (MD) simulations.[1–4] The chemical reaction and the associated bond formation is triggered by a simple distance criterion between two reactive particles. The method has been successfully applied to chain propagation of linear polystyrene[4] and curing reactions of an epoxy system[2,5]. These early experiences raised the question if such an approach can also be used to mimic entanglement coupling in polymer melts. The bond formation algorithm could be used to insert cross-links between polymer chains, like in a polymeric network. However, the cross-links would need to possess a certain mobility to incorporate the full viscoelastic behavior of entangled polymer melts. The first attempts were carried out during my diploma thesis. The so-called slip-springs led to a reduction of the chain mobility. However, the model as a whole failed to reproduce the famous scaling laws for the dynamical properties[6] - and even worse - the slip-springs affected the chain statistics[7]. These initial problems have been eliminated during my Ph.D. thesis and since then, the model has proven its applicability to a variety of systems.[8–10]

Polymeric systems are of high industrial importance due to their ubiquitous role in everyday life. It is of tremendous interest to understand, how to control their mechanic properties for the development of new commodities. Polymeric products usually consist of not only a single well-defined component but rather of a mixture of various polymer chains. The purpose of polymer blending is to combine some advantageous properties of the individual components in a single system. This way, the properties of the material can be tailor-made to meet the requirements for a specific application. However, the underlying principles of polymer-blending are not exactly understood. Thus polymer blending is often done through trial and error which is costly in terms of time and money. Particle-based computer simulations might provide us with a better insight into the dynamical mechanisms, especially in situations where theoretical or experimental options have reached their limits. Computer simulations have several decisive advantages over experiments. They allow the setup of a perfect, well-defined system without impurities. The chain lengths can be exactly specified with a determined polydispersity. Interactions can be chosen and tuned at will. In experiments this is only possible to a very limited extend. Furthermore, the microscopic description of the molecules opens up experimentally inconceivable options for a more detailed analysis. However, the simulations have difficulties to consider entanglements in polymer chains

properly.[11] The reason will be discussed thoroughly below. Entanglements affect the rheological properties of the material greatly because they reduce the dynamics of the chains.[6] An entanglement is often visualized in textbooks as a knot or a coil of chains, similar to the noodles in a bowl of cooked spaghetti. Strictly speaking, however, an entanglement is defined by experimental measures.[12] The chains in a polymer melt overlap heavily if their length exceeds a chemically determined critical length. For long time-scales the melt behaves like a viscous fluid while for short time-scales it behaves like an elastic network. This retardation in chain dynamics has been attributed to temporary coupling effects between the chains.[6] These effects significantly reduce the chain motion and are the cause for the viscoelastic behavior. A polymer melt which exhibits these coupling effects is referred to as entangled.[12]

The tube model which has later been refined by reptation theory, is an analytical approach that predicts the dynamics of an entangled probe chain.[6,13] It is a single-chain model, defined in terms of four parameters. These are the number of beads, the Kuhn segment length between the beads, the monomeric friction coefficient and the tube diameter. The first three parameters already appear in the formulation of the Rouse model[14]. The additional parameter, the tube diameter, is of special importance as it defines the entanglement spacing.[6] The tube model consists of a single chain confined by topological constraints that are fixed in space. The chain is prohibited to cross the obstacles and therefore, can only move within this tube. Consequently, stress relaxation of the single chain occurs only through a curvilinear motion along the tube axis. This motion out of the tube resembles the slithering of a snake, which is why it is called reptation dynamics. The model assumes that neighboring chains in a polymer melt restrict the chain dynamics in the same manner as these obstacles. The predictions made by the original tube model are close to experimental observations. However, the simplifications are too rigorous to account for the complicated and versatile relaxation mechanisms. The model is not self-consistent as it assumes that the obstacles are fixed in space with infinite lifetime. After all, since the obstacles are imposed by the surrounding chains, their position should change with time as the neighboring chains are moving around.[15,16] These multi-chain effects are difficult to take into account in a single-chain model. Therefore, over the last decades the tube model has been continuously further developed to consider more and more relaxation processes under flow and equilibrium.[17–20] The model is now able to predict quantitatively the experimentally found scaling laws for the diffusion coefficient or viscosity in melts of linear polymer chains. Furthermore, it reproduces the relaxation modulus and linear viscoelasticity of the entangled chains. The concept has also been extended to polydisperse systems[15,16] or star polymers[21] where the concept of “arm

retraction" could explain the diffusion behavior. However, multi-chain effects and the flow-behavior are still unsolved problems and the model cannot describe interfaces.

Up to this date, full atomistic Molecular Dynamics (MD) simulations are inapplicable to study the dynamics of entangled polymer chains.[11] The simulations are very time-consuming because the fast internal degrees of freedom make it necessary to calculate the interactions every few femtoseconds. Even for relatively short chains with only a few hundred monomer units, the characteristic times to observe the entanglement behavior are in the range of nanoseconds or picoseconds. An additional problem are the characteristic times, which scale with the molecular weight with an exponent of 3.4.[6] As a consequence, the required simulation time increases more than tenfold when the chain length is doubled. Another aspect is the system size which has to be enlarged with the chain length in order to avoid interactions of a chain with itself through the periodic boundary conditions of the simulation cell.[22] A coarse-grained (CG) modeling of the polymer chains is an appealing and frequently used way to extend the accessible time-scales in MD simulations.[23] The principle is to simplify the computation by neglecting certain degrees of freedom, which are assumed to be unnecessary. In the united atom model, for instance, the number of degrees of freedom is reduced by grouping carbon atoms together with their chemically bonded hydrogen atoms. Harmandaris et al. used a united atom model of linear polyethylene chains with increasing chain lengths to show the crossover from unentangled to entangled dynamics.[24] In this spirit, it is possible to lump several atoms or even an entire monomer into a single CG-bead.[11,23] However, the repulsive potential of the CG-beads becomes softer with the number of grouped atoms, in order to retain the structure of the full atomistic molecule. The trajectory of an atom is usually disturbed by frequent collisions with other surrounding atoms. Collisions of the CG-beads, however, are too weak and do not lead to a constant change in momentum. Additional stochastic forces as in Brownian Dynamics (BD)[25] or Dissipative Particle Dynamics[26,27] (DPD) become necessary to imitate these collisions with hard-sphere objects. The entanglement coupling is still observable, if the repulsive force between the particles is strong enough to prevent unphysical bond crossings. The Kremer-Grest (KG) model[28] is the most coarse-grained representation of a chain that still accounts for entanglements by excluded volume effects. The combination of hard-sphere Lennard-Jones potentials with finite extensible bonds ensures that the chains cannot cross each other. The KG model is able to reproduce the scaling behavior of several dynamical properties[28] as well as the stress relaxation of entangled melts[29]. The chemical identity of the molecules vanishes for highly coarse-grained representations. The bead-spring chains in KG simulations cannot be assigned to a specific polymer anymore as they have lost all of their chemical identity through the

coarse-graining procedure. Hence, highly coarse-grained polymer chains are suitable only for measures of generic properties and do not account for the atomistic details.[30]

A serious problem arises for the dynamic properties of chains that use a coarse grained modeling higher than in KG simulations. The chains can pass through each other due to the soft nonbonded potentials. As a result of these unphysical bond crossings, the melt does not exhibit entangled behavior anymore. This is usually the case for DPD simulations, where it is not uncommon that an entire chain segment is grouped to a single interaction site.[31] Some approaches retain the uncrossability constraints of the chains by means other than excluded volume interactions. The Twentanglement algorithm uses elastic bonds that prevent chain penetration.[32] However, it is rather time-consuming and difficult to implement in the code. The Segmental Repulsive Potential algorithm introduces a repulsive force between springs to keep them apart.[33] The Bond Fluctuation model[34] belongs to the group of lattice models. Discrete moves that would lead to a violation of the chain uncrossability are simply prohibited but the method is usually restricted to lower polymer densities.

Quite different are the slip-link and slip-spring simulations which allow chain crossings.[35–38] They recover the entanglement effect by the insertion of new, artificial constraints. The entanglement coupling is mimicked by artificial constraints. This idea has been derived from the common view of an entanglement as a knot between two chains and is not based on theoretical considerations. The intention of this model is to reproduce the experimental behavior of entangled polymer chains. Then the model can be applied to systems in which the entangled dynamics of the chains is important for the behavior. Its primary purpose is not to learn more about entanglements itself. For this, the model is rather unsuitable because of the lack of a theoretical foundation. In this spirit, various models have been developed that are overall quite successful to reproduce the rheological behavior.[39,40] The slip-link model has been firstly introduced by Hua and Schieber.[35] The actual entangled polymer is modeled by a chain of Brownian particles that is constrained by network nodes (i.e. slip-links). The slip-links are created and destroyed through the sliding motion at the chain ends. Constraint release effects are taken into account by different ways of pairing between slip-links. The primitive chain network model of Masubuchi et al. is a multi-chain version of the slip-link.[38] The slip-links are bundling the chains together to form a network. Likhtman developed a single chain slip-spring model, where a chain is constrained to fixed positions in space through a spring.[36] The model has later been transformed to a multi-chain version by Uneyama and Masubuchi.[37] A higher coarse-grained modeling that goes beyond the slip-links or slip-springs simulations is used in the RaPiD model of Kindt and Briels[41]. There, the entire

chain is represented by only a single particle. The retardation due to entanglements is taken into account by parameters that depend on the overlap of the chains.

The slip-spring model proposed within this thesis belongs to the multi-chain simulations.[8–10] Its major advantage compared to the other methods is the utilization of the DPD thermostat.[27] The DPD thermostat is an extension of the Langevian thermostat and is capable of conserving the momentum locally. Hence, it is the thermostat of choice whenever hydrodynamic interactions become important. In particular, this is the case for polymer solutions where momentum must be transported through the solvent molecules. Its integration scheme is very stable and might be used for shearing simulations as well.[42] The only disadvantage of DPD is that it is computational less efficient than other thermostats. The reason is that the dissipative force requires the calculation of velocity differences. The required calculation of the velocity vectors also increases the amount of communication for parallelized codes that use the domain decomposition method.[43] Entanglements are mimicked by harmonic springs between beads of nearby chains. These slip-springs differ from cross-links in a polymeric network by their ability to migrate along the chain from bead to bead. The slip-spring can be destroyed if one of the two mounting points reaches a chain end. After its destruction, the slip-spring must be newly created at another randomly selected chain end such that the number of slip-springs remains constant. The simulation alternates between sequences of DPD and Monte Carlo (MC) steps[25]. The chain bead dynamics is calculated during the DPD sequences, while the slip-spring positions are fixed. Vice versa, the slip-spring dynamics is considered during the MC sequences, while the bead position is fixed. This way, the dynamics of the chain beads and slip-springs is treated separately. Chappa et al.[44] have developed a very similar model that also makes use of the combination of slip-springs and DPD thermostat.

The number of slip-springs is an important input parameter of the slip-spring simulation and determines the entanglement length of the chains. This length scale is originally defined by the tube model. Its microscopic interpretation is the number of monomers between two consecutive entanglements along the chain. The entanglement length of real polymers is chemistry dependent and mostly determined by the chain stiffness. Lengths of up to a few hundred monomers are realistic values for experimental polymer chains.[28] However, it can also be much shorter as for polycarbonate with a length between 5 and 8 repeating units.[45] The entanglement length can be extracted from experiments or simulations in various ways.[28,45,46] It is often obtained from viscoelastic data using a relation from tube theory that links the plateau value with the entanglement length.[6] Alternatively it can also be measured through the diffusion coefficient or the dynamic structure factor. The different approaches yield a wide range of entanglement lengths. For molecular simulations there is the additional

possibility to obtain the entanglement length directly from the chain conformation in a melt. For a given snapshot the chain ends are fixed in space and the temperature is reduced to 0 K. The chains tighten as a result of the temperature decrease but may not violate the uncrossability constraints. At the end, the taut chains are representing the primitive path, which is the shortest connection between the chain ends without crossing any other chains. The entanglement length is then the number of monomers per Kuhn segment of the primitive path. Besides the mentioned primitive path analysis[30], there are also two other algorithms called Z1[47] and CReTA[48] which work in similar ways. The simulations and models that have been introduced so far can be compared with each other or mapped onto experimental results. Kremer and Grest compared his bead-spring model with experimental results and the tube model.[28] Likhtman mapped the parameter of his single-chain slip-spring model to agree with different experimental techniques of various polymer species and the tube model.[36]

My thesis is structured as follows. The second chapter introduces the algorithm in detail and provides a basic introduction of the DPD simulation technique[26,27]. The method is verified for the simplest case: a melt of monodisperse, linear polymer chains. The slip-spring density is chosen such that on average every fifth bead is connected with a slip-spring. This way, the longest chains in the system have about 20 slip-springs and can be considered as moderately entangled. We compare several aspects of the chain dynamics with the analytical solutions of the tube model.[6] For the simulations without slip-springs we observe Rouse behavior regardless of the chain length as expected for polymer chains that have no entanglements.[31] For the simulations with slip-springs we can see a transition in the behavior from unentangled to entangled dynamics, i.e. from Rouse to reptation dynamics, as the chain length exceeds a critical threshold value. The behavior predicted by our method is compared with results from Kremer-Grest simulations to estimate the gain in computational speed over conventional methods that use excluded volume interactions to ensure uncrossability of the chains. The next chapter is about the dynamics of bidisperse polymer melts, i.e. a melt with two different chain lengths.[15,16] It has been observed experimentally that the resulting performance of a polymer blend is not just a simple combination of the properties of the single species. In fact, the fast relaxation of the short chains accelerates the dynamics of the long chains and vice versa. The tube model has been extended to account for these multi-chain effects. However there is still no consensus as two competing theories make different assumptions and hence, come to different conclusions.[15,16] Experiments usually have trouble to measure the dynamic properties for only one chain length, while neglecting the other. The slip-spring model has been applied to the bidisperse systems without any modifications. The system size is much larger than in the previous chapter to ensure good statistics even for

systems where the density of the long chain component is low. We compare our results with Kremer-Grest simulations and find a quantitatively similar behavior. The results encouraged us to take a closer look on the multi-chain relaxation mechanisms constraint-release and tube-dilation.[15,49] The fourth chapter critically tests the applicability of the model in polymer solutions. The solvent molecules are represented by unconnected DPD beads. The nonbonded interactions of the chain beads and the solvent beads are identical, such that the system can be regarded as polymer chains in theta-solution[7]. The volume fraction of the solvent ranges from dilute to concentrated polymer solutions. The total number of slip-springs scales with the polymer concentration. We measure the linear viscoelasticity and illustrate the onset of the entanglement coupling at increasing polymer concentration. The simulations of various chain lengths and polymer concentrations are consistent with each other and with experiments.[50,51] The last chapter concludes with a brief summary of the results. The model has been developed as a loophole to simulate entangled polymer dynamics for highly coarse-grained polymer chains. So far we have focused mostly on the validation of the slip-spring model for a few systems of interest. Thus, the last section will also provide an outlook for future studies with a few suggestions of other systems that would be interesting to examine.

References:

[1] K. Farah, F. Leroy, F. Müller-Plathe, and M.C. Böhm, J. Phys. Chem. C **115**, 16451 (2011).

[2] K. Farah, M. Langeloth, M.C. Böhm, and F. Müller-Plathe, J. Adhes. **88**, 903 (2012).

[3] K. Farah, F. Müller-Plathe, and M.C. Böhm, ChemPhysChem **13**, 1127 (2012).

[4] K. Farah, H.A. Karimi-Varzaneh, F. Müller-Plathe, and M.C. Böhm, J. Phys. Chem. B **114**, 13656 (2010).

[5] M. Langeloth, T. Sugii, M.C. Böhm, and F. Müller-Plathe, Soft Mater. **12**, 71 (2014).

[6] M. Doi and S.F. Edwards, *The Theory of Polymer Dynamics* (Oxford University Press, 1986).

[7] M. Rubinstein and R.H. Colby, *Polymer Physics* (Oxford University Press, 2003).

[8] M. Langeloth, Y. Masubuchi, M.C. Böhm, and F. Müller-Plathe, J. Chem. Phys. **138**, 104907 (2013).

[9] M. Langeloth, Y. Masubuchi, M.C. Böhm, and F. Müller-Plathe, J. Chem. Phys. **141**, 194904 (2014).

[10] M. Langeloth, Y. Masubuchi, M.C. Böhm, and F. Müller-Plathe, Macromolecules **submitted**, (2015).

[11] J.T. Padding and W.J. Briels, J. Phys. Condens. Matter **23**, 233101 (2011).

[12] Y. Masubuchi, Annu. Rev. Chem. Biomol. Eng. **5**, 11 (2014).

[13] P.G. de Gennes, J. Chem. Phys. **55**, 572 (1971).

[14] P.E. Rouse, J. Chem. Phys. **21**, 1272 (1953).

[15] J.L. Viovy, M. Rubinstein, and R.H. Colby, Macromolecules **24**, 3587 (1991).

[16] M. Doi, W.W. Graessley, E. Helfand, and D.S. Pearson, Macromolecules **20**, 1900 (1987).

[17] S.T. Milner and T.C.B. McLeish, Phys. Rev. Lett. **81**, 725 (1998).

[18] H. Watanabe, Y. Matsumiya, and E. Van Ruymbeke, Macromolecules **46**, 9296 (2013).

[19] C. Pattamaprom and R.G. Larson, Macromolecules **34**, 5229 (2001).

[20] G. Marrucci, J. Nonnewton. Fluid Mech. **62**, 279 (1996).

[21] P.G. De Gennes, J. Phys. **36**, 1199 (1975).

[22] Y.R. Sliozberg, T.W. Sirk, J.K. Brennan, and J.W. Andzelm, J. Polym. Sci. Part B Polym. Phys. **50**, 1694 (2012).

[23] F. Müller-Plathe, ChemPhysChem **3**, 754 (2002).

[24] V.A. Harmandaris, V.G. Mavrantzas, D.N. Theodorou, M. Kröger, J. Ramírez, H.C. Ottinger, and D. Vlassopoulos, Macromolecules **36**, 1376 (2003).

[25] D. Frenkel and B. Smit, *Understanding Molecular Simulation: From Algorithms to Applications* (Academic Press, 2002).

[26] P.J. Hoogerbrugge and J.M.V.A. Koelman, Europhys. Lett. **19**, 155 (1992).

[27] R.D. Groot and P.B. Warren, J. Chem. Phys. **107**, 4423 (1997).

[28] K. Kremer and G.S. Grest, J. Chem. Phys. **92**, 5057 (1990).

[29] A.E. Likhtman, S.K. Sukumaran, and J. Ramirez, Macromolecules **40**, 6748 (2007).

[30] R. Everaers, S.K. Sukumaran, G.S. Grest, C. Svaneborg, A. Sivasubramanian, and K. Kremer, Science **303**, 823 (2004).

[31] N.A. Spenley, Europhys. Lett. **49**, 534 (2000).

[32] J.T. Padding and W.J. Briels, J. Chem. Phys. **115**, 2846 (2001).

[33] G. PAN and C.W. MANKE, Int. J. Mod. Phys. B **17**, 231 (2003).

[34] I. Carmesin and K. Kremer, Macromolecules **21**, 2819 (1988).

[35] C.C. Hua and J.D. Schieber, J. Chem. Phys. **109**, 10018 (1998).

[36] A.E. Likhtman, Macromolecules **38**, 6128 (2005).

[37] T. Uneyama and Y. Masubuchi, J. Chem. Phys. **137**, 154902 (2012).

[38] Y. Masubuchi, J.I. Takimoto, K. Koyama, G. Ianniruberto, G. Marrucci, and F. Greco, J. Chem. Phys. **115**, 4387 (2001).

[39] C. Tzoumanekas and D.N. Theodorou, Curr. Opin. Solid State Mater. Sci. **10**, 61 (2006).

[40] J.D. Schieber and M. Andreev, Annu. Rev. Chem. Biomol. Eng. 367 (2014).

[41] P. Kindt and W.J. Briels, J. Chem. Phys. **127**, (2007).

[42] T. Soddemann, B. Dünweg, and K. Kremer, Phys. Rev. E **68**, (2003).

[43] S. Plimpton, J. Comput. Phys. **117**, 1 (1995).

[44] V.C. Chappa, D.C. Morse, A. Zippelius, and M. Müller, Phys. Rev. Lett. **109**, 148302 (2012).

[45] K. Kremer, S.K. Sukumaran, R. Everaers, and G.S. Grest, in *Comput. Phys. Commun.* (2005), pp. 75–81.

[46] M. Pütz, K. Kremer, and G.S. Grest, Eur. Lett. **49**, 735 (1999).

[47] M. Kröger, Comput. Phys. Commun. **168**, 209 (2005).

[48] C. Tzoumanekas and D.N. Theodorou, Macromolecules **39**, 4592 (2006).

[49] Y. Matsumiya, K. Kumazawa, M. Nagao, O. Urakawa, and H. Watanabe, Macromolecules **46**, 6067 (2013).

[50] Y. Heo and R.G. Larson, Macromolecules **41**, 8903 (2008).

[51] Q. Huang, O. Mednova, H.K. Rasmussen, N.J. Alvarez, A.L. Skov, K. Almdal, and O. Hassager, Macromolecules **46**, 5026 (2013).

THE JOURNAL OF CHEMICAL PHYSICS **138**, 104907 (2013)

Recovering the reptation dynamics of polymer melts in dissipative particle dynamics simulations via slip-springs

Michael Langeloth,[1,a)] Yuichi Masubuchi,[2] Michael C. Böhm,[1] and Florian Müller-Plathe[1]
[1]*Eduard-Zintl-Institut für Anorganische und Physikalische Chemie and Center of Smart Interfaces, Technische Universität Darmstadt, Petersenstr. 20, D-64287 Darmstadt, Germany*
[2]*Institute for Chemical Research, Kyoto University, Gokasho, Uji 611-0011, Japan*

(Received 13 November 2012; accepted 20 February 2013; published online 14 March 2013)

We report a multi-chain approach for dissipative particle dynamics where the uncrossability constraints of polymer chains are mimicked by temporary cross-links, so-called slip-springs. The conformational statistics of the chains are not affected by the introduction of slip-springs. Dynamical properties such as mean square displacements, diffusion coefficient, and longest relaxation time are in good agreement with the results of reptation theory. According to our analysis, the present formalism is 500 times faster and requires 7 times fewer beads than conventional generic polymer models employing Newtonian dynamics and excluded-volume potentials. © *2013 American Institute of Physics*. [http://dx.doi.org/10.1063/1.4794156]

INTRODUCTION

The dynamics of a chain in a polymer melt can be described by two different theories. The Rouse model[1] provides excellent results for sufficiently short chains but fails to reproduce the long-time motion of chains whose molecular weight exceeds a certain critical value M_c.[2] For such chains, the surrounding melt confines each chain via topological constraints called entanglements. However, they do not feel these constraints immediately. At first, each chain follows the Rouse model like a chain in free space until it realizes its confinement. This onset of the entanglement effect is denoted as the entanglement time τ_e beyond which the Rouse model is no longer valid. The reptation model accounts for this confinement.[3] It allows only lateral motion of the chain along its own contour, which resembles that of a slithering snake; hence, the name reptation model. In this scheme, the lateral motion is less efficient in relaxing stress or the orientation of the chains. The crossover from Rouse to reptation dynamics with the associated deceleration can be reproduced by atomistic or weakly coarse-grained (CG) polymer simulations. CG methods reduce the number of degrees of freedom by lumping several atoms into a single bead, thereby facilitating simulations of much longer time and length scales.[4] The hard-core potentials of the particles prevent mutual crossings of the chains. The individual chain is thus confined by the surrounding polymer melt in the same manner as postulated by the reptation model. These uncrossability constraints are the dominant factor for the slowing down of the chain dynamics. Entanglement effects have been demonstrated for the first time by the Kremer-Grest (KG) model,[5] a generic approach where finite extensible nonlinear elastic chain springs are adjusted to a Lennard-Jones potential in such a way as to prevent bond crossings. Such simulations are, however, not always feasible for longer chain lengths due to an explosion of time and length scales. This becomes obvious when one considers that the rotational relaxation time τ_{rot} of a chain scales with N^3, where N is the chain length.[2] In contrast, unphysical bond crossings are no longer prevented by excluded volume effects when the polymer is coarse-grained beyond a certain level.[6] This follows from the soft nature of the highly coarse-grained potentials. As a consequence, the entanglement effect is lost. Thus, the chain motion becomes accelerated and follows a qualitatively different dynamics. Hence, the absence of these topological constraints may cause an unrealistic rheology of the system.

Several attempts to reintroduce the entanglement effect to highly coarse-grained simulations have been reported.[7–10] Here, we introduce an approach that is based on the single-chain slip-spring model of Likhtman[7] and on the primitive chain network (PCN) formalism of one of the present authors.[11] Our model is built on a multi-chain approach, where chain beads are temporarily cross-linked by so-called slip-springs. Hereby, it does not matter whether the two connected beads belong to different chains or not. These auxiliary interactions successfully compensate the loss of the uncrossability constraints and the associated entanglement effect. The slip-springs can move along the chain in discrete steps from bead to bead. Moreover, slip-springs may also relocate from one chain end to another. The migration and relocation are both governed by different Metropolis Monte Carlo (MC)[12] sequences that both ensure detailed balance.[9] This condition is required to obtain proper equilibrium distribution. In the present study, we chose dissipative particle dynamics (DPD)[13] for the computation of the particle dynamics because it allows highly CG models with soft-core potentials and very long timesteps. Thus, our simulations alternately switch between short DPD and MC sequences to compute the dynamics of the particles and the slip-springs, respectively. Our approach is different from earlier studies where the uncrossability between chains is restored by tuning the inter-bead interaction in the DPD scheme. Pan and Manke[14] have proposed a modification of the DPD force to reduce the frequency of chain

a)Author to whom correspondence should be addressed. Electronic mail: m.langeloth@theo.chemie.tu-darmstadt.de.

crossings by a segmental repulsion. Similar tunings on the inter-particle interaction have been adopted by other research groups, too.[15–17] An alternative has been to modify the DPD equations of motion to prohibit chain crossing.[10]

We like to pursue here a different approach where the motional constraints for the chain dynamics are not generated by the inter-bead interaction, but are introduced *a priori* by slip-springs. Other slip-spring like approaches have been developed independently by different groups: Chappa *et al.*[8] have very recently reported a model using DPD for the bead motion and MC for the slip-spring dynamics including slippage, creation, and destruction. Uneyama and Masubuchi[9] have developed a dynamical scheme derived from the total free energy of the system. Our model is similar to these recent developments, especially to the approach by Chappa *et al.*[8] (although our model has been developed independently from other works). In addition to differences in the models used to combine soft-core particle dynamics with Monte Carlo slip-link dynamics, we have characterized the chain dynamics of our approach in different ways. We demonstrate that our method is capable of reproducing the correct scaling behavior for the diffusion up to a chain length of 150 beads. Additionally, we carefully examine the consequences of monomer retardation and provide an analysis of stress and orientational relaxation. In the end, the computational speed of our scheme is compared with the KG model as a "standard" example of the hard-core-Newtonian-dynamics models.

MODEL

We consider dense melts of polymer chains. The entanglement among the polymers is mimicked via slip-springs, each of which connects beads either between or within a chain and is able to slide along them. The dynamics of the system consists of (a) motion of the beads described by DPD, (b) formation and termination of the slip-springs according to a MC scheme, and (c) sliding of the slip-springs ruled by another MC scheme. Details of each scheme are explained below. The DPD method[13] follows a stochastic equation of motion, which conserves momentum, and is suitable for hydrodynamic studies, too. The force exerted on a particle i by all other particles j has the following form:

$$\overrightarrow{F_i} = \sum_{i \neq j} \overrightarrow{F_{ij}^C} + \overrightarrow{F_{ij}^D} + \overrightarrow{F_{ij}^R}, \tag{1}$$

where $\overrightarrow{F_{ij}^C}$, $\overrightarrow{F_{ij}^D}$, and $\overrightarrow{F_{ij}^R}$ are conservative, dissipative, and random force, respectively. Dissipative and random forces obey the fluctuation dissipation theorem[18] (Eq. (2)) and thus cannot be chosen independently

$$\sigma^2 = 2\gamma k_B T. \tag{2}$$

The value γ is the friction parameter for $\overrightarrow{F_{ij}^D}$, σ the noise amplitude for $\overrightarrow{F_{ij}^R}$, k_B the Boltzmann constant, and T the temperature. The nonbonded conservative force $\overrightarrow{F_{ij}^C}$ is soft-core, purely repulsive, and decreases linearly with distance r_{ij} up to a cut-off radius r_c,

$$\overrightarrow{F_{ij}^C} = a_{ij}\left(1 - \frac{r_{ij}}{r_c}\right)\overrightarrow{e_{ij}} \quad \text{if} \quad r_{ij} < r_c, \tag{3}$$

where a_{ij} is the repulsion parameter. To model linear polymer chains, we introduce a linear attractive spring force $\overrightarrow{F_i^B}$ (Eq. (4)) that connects two adjacent beads i and j with a weak spring constant k

$$\overrightarrow{F_i^B} = \sum_j k\overrightarrow{r_{ij}}. \tag{4}$$

For the integration scheme, we employ a modified version of the velocity-Verlet algorithm as proposed by Groot and Warren.[19] More detailed accounts on DPD can be found in the same reference. Slip-springs are placed initially between randomly chosen pairs of beads under the condition that their distance is within $r_c/2$ and $2r_c$. Afterwards, their connection is equilibrated via the slip-spring dynamics explained below.

The pair of beads may or may not belong to different chains. Thus, inter- and intra-chain slip-springs are likewise considered in this formalism. They are modeled like regular chain bonds with the same attractive force $\overrightarrow{F_i^B}$. The position of the slip-springs is fixed during a DPD sequence. The system would behave like an elastomeric network, rather than a polymer melt, if there were no MC steps to move the slip-springs along both chains. At every single MC step, the algorithm goes through all slip-springs sequentially and attempts to shift both mounting points by one bead. The shift direction is chosen independently for both mounting points and with equal probability either to the right or left side along the chain. The trial moves are accepted if the Metropolis criterion is fulfilled and rejected if not. Thus, the Metropolis criterion ensures detailed balance.[9] The slip-spring motions are completely independent of each other and there are no interactions between slip-springs whatsoever. Thus, a single bead can hold more than one slip-spring at a time, and slip-springs can pass through each other. Intra-chain slip-springs might come closer to each other during the entanglement migration until they both fall onto the same bead. In such rare cases, the slip-spring is immediately removed and created elsewhere to avoid the formation of entanglement knots. Except for these intra-chain slip-spring collapses, no other relocations of slip-springs are allowed during the MC sequence. We deploy the same mechanism as for the initial setup of slip-springs (described above) to select a different pair of beads for the new slip-spring position. The ratio of DPD and MC steps must be chosen carefully to obtain the expected dynamical properties of the chains. Our observations reveal that the chain motion is too much suppressed by slip-springs if the relative number of MC steps is below a certain threshold value. In the borderline case of zero slip-spring mobility, the entangled polymer melt would behave more like an elastomeric network as it was mentioned before. A more thorough discussion on that issue is provided in the Appendix. Since bead and slip-spring dynamics are treated separately by different processes, we infer that these processes must be balanced such that the bead and slip-spring dynamics are consistent with each other. Hence, we use

the relaxation time τ_{SS} of a slip-spring to compare the evolution during a DPD and a MC sequence. The relaxation time was hereby derived from the autocorrelation function $\Theta(t)$ of the slip-spring bond vector $\vec{P}(t)$ at time t

$$\Theta(t) = \frac{\langle \vec{P}(t) \cdot \vec{P}(0) \rangle}{\langle P^2 \rangle}. \quad (5)$$

We fitted $\Theta(t)$ to single exponential decay function in the long time regime and obtained the longest relaxation time as τ_{SS} for DPD and MC sequences separately. As it turns out, τ_{SS} is almost the same for DPD and MC sequences when we chose the same number of steps for DPD and MC sequences (n_{DPD} and n_{MC}, respectively). A second MC algorithm enables all slip-springs that have reached at least one chain end to relocate to another chain end. In this process, the new slip-spring is formed between an arbitrarily chosen chain end and a neighboring bead with the same distance criterion as used for the initial creation of slip-springs. Again, the Metropolis criterion decides if the relocation is accepted or rejected and guarantees that this process obeys the detailed balance condition, too. In this respect, every slip-spring with at least one mounting point located at a chain end is given the opportunity to relocate only once after each completed DPD sequence. The average number of slip-springs that successfully undergo relocation after every DPD sequence divided by the number of chains in the melt is called α. Since formation and termination of slip-springs are carried out simultaneously during the relocation process, the number of slip-springs at an individual chain may vary as a function of time but their total number is always constant. This is an important simplification in comparison to the approach proposed by Chappa *et al.*[8] or Uneyama and Masubuchi[9] where the number of slip-springs is controlled by a chemical potential whose physical meaning seems to be somewhat ambiguous.

The rate of formation and termination of entanglements has been chosen as $1/\tau_e$, where τ_e is the relaxation time of a chain segment between slip-springs. In this way, we ensure that the equilibration of the entanglement topology and the chain conformation are consistent. The average time for a single relocation per chain equals n_{DPD}/α in our model. Since neither α nor τ_e depend on n_{DPD} or N we can easily adjust n_{DPD} such that a single slip-spring relocation per chain occurs every τ_e.

The entire algorithm of the presented simulation is summarized below.

I. Slip-springs are created in the beginning of the simulation using a distance criterion.
II. One MC sequence (n_{MC} steps): Slip-springs can migrate along the chain. However, they cannot relocate to other chains, even though they may reach a chain end.
III. Start of the main loop:
   (a) One DPD sequence (n_{DPD} steps): Bead dynamics. The mounting points of the slip-springs are fixed (i.e., no migration or relocation processes).
   (b) Relocation of slip-springs: Slip-springs that are at a chain end may move to another randomly selected chain end under the condition that the Metropolis criterion is fulfilled for this move.
   (c) One MC sequence (n_{MC} steps): Same as in II.
IV. The simulation is terminated when the total simulation time (in units of DPD steps) is reached.

SIMULATION DETAILS

We consider a melt of monodisperse linear chains modeled by the optimized DPD parameters described in the article of Groot and Warren.[19] We work in reduced units such that energy, mass, and length are scaled to unity, hence, $k_BT = m = r_c = 1$; this entails a time unit of $t_{DPD} = (r_c{}^2 m/k_BT)^{0.5} = 1$. The total number of beads is 3000 for all simulations and the chain length N ranges from 5 to 150 beads. The cubic periodic box has a constant length of 10 r_c, whereby all simulations were carried out at a number density of $\rho = 3\ r_c{}^{-3}$. We use the typical values for the repulsion parameter $a_{ij} = 25\ k_BT$ and the spring constant $k = 2\ k_BT/(r_c)^2$. With these parameters, our system yields the same compressibility as water, which is a suitable reference for various polymers.[19] The integration is performed with a timestep of $\Delta t = 0.06\ t_{DPD}$. The noise amplitude for the thermostat is set to $\sigma = 3\ k_BT(t_{DPD})^{0.5}/r_c$.

The introduction of slip-springs requires a few more parameters that determine the degree of entanglement and the speed at which slip-springs move along the chain or relocate to other chains. The constant number of slip-springs is 300 for all chain lengths. This choice corresponds to N_e (the average segment number between two entanglements) close to 5 beads. The average number of successful slip-spring relocations per chain α was found to be 0.13. In addition, the analysis of the mean square displacement of the central bead $g_{1,mid}(t)$ indicates that the entanglement effect occurs at approximately $\tau_e = 4000$ timesteps. This will be discussed within the Results section in more detail (Figure 3). Since $\tau_e = n_{DPD}/\alpha$ and $n_{DPD} \sim n_{MC}$ (as explained in the Model section), we choose $n_{DPD} = n_{MC} = 500$. Altogether, we repeatedly perform sequences of 500 DPD and 500 MC steps until we have reached the total simulation time. Relocation of slip-springs is carried out in between a DPD and MC sequence. The simulation time is reported in units of DPD steps, i.e., MC and relocation steps do not enter the determination of time in dynamical quantities.

RESULTS

Chain structure

The radius of gyration of a Gaussian chain scales with the chain length as $\langle R_g^2 \rangle \propto N^1$ regardless of topological constraints. Figure 1(a)) shows $\langle R_g^2 \rangle$ as a function of the chain length N in a double logarithmic scale for unentangled chains (empty symbols) and our slip-spring model (filled symbols). We obtain the same qualitative and quantitative results for our slip-spring model and the classical DPD simulation. Therefore, we conclude that slip-springs do not significantly affect the structural properties of the chains. In addition, we show the intermonomer distance d(s) of a chain with length $N = 100$ in Figure 1(b). Here, d(s) represents the mean squared end-to-end distance of a chain segment with the length s.[16] The plot confirms our previous statement and shows that the

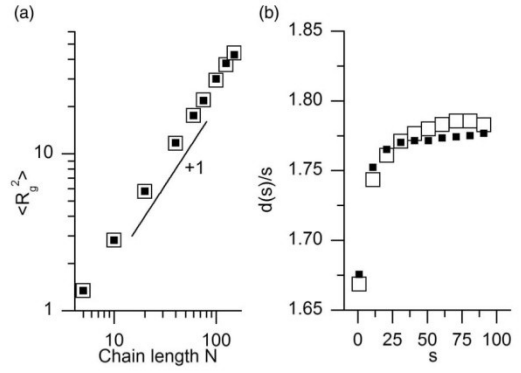

FIG. 1. Measures of the chain structure: (a) Radius of gyration $\langle R_g^2 \rangle$ plotted against N. The line with slope +1 is a guide to the eye to show agreement with the scaling law. (b) Mean square internal distance d(s) for the chain length $N = 100$ scaled by the bead distance s. Empty symbols illustrate the system without slip-springs, i.e., classical DPD simulation. Filled symbols show the behavior of the system with slip-springs.

deviations of the simulation with slip-springs (filled symbols) and classical DPD simulation without slip-springs (empty symbols) are negligibly small. Formation of slip-springs inevitably leads to a slight pressure reduction due to the introduction of an additional attractive force which might affect the static properties of the chains. For this reason, Uneyama and Masubuchi[9] as well as Chappa *et al.*[8] recently reported the need for a correction term which compensates the attractive spring potential in their slip-spring models. However, this appears to be negligible in the present DPD simulation because the overall attractive contribution of the weak entanglement springs to the pressure is sufficiently small in contrast to the stronger repulsive conservative force. It is not certain, though, that this is still valid for less dense systems or stronger entanglement springs.

Dynamics

Figures 2 and 3 show the mean square central monomer displacement $g_{1,mid}(t)$ for chains without (dashed lines) and with slip-springs (solid lines) for four different chain lengths

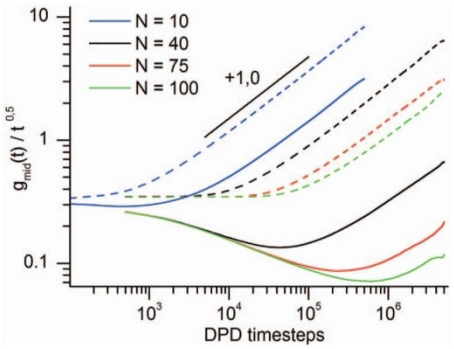

FIG. 2. Mean square displacement of the central bead $g_{1,mid}(t)$ scaled by $t^{1/2}$ for chains without (dashed curves) and with slip-springs (solid curves). The chain length N varies from 10 to 100. The line is a guide to the eye and shows the t^1 regime.

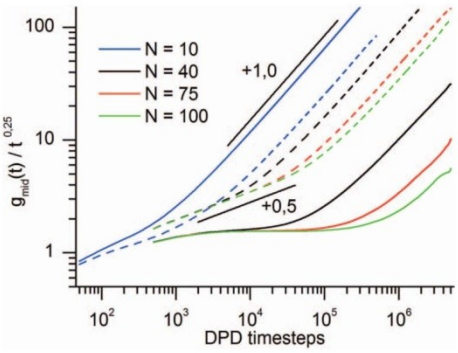

FIG. 3. Mean square displacement of the central bead $g_{1,mid}(t)$ scaled by $t^{1/4}$ for chains without (dashed curves) and with slip-springs (solid curves). The chain length N varies from 10 to 100. The two lines are guides to the eye and show the t^1 and $t^{1/2}$ regime, respectively.

N. Figure 2 is scaled by $t^{1/2}$ and Figure 3 by $t^{1/4}$ in order to emphasize two different diffusive regimes. Short chains ($N = 10 \approx 2\ N_e$) with slip-springs reveal a transition from a $t^{1/2}$ to a t^1 regime and thus, show the same Rouse-like behavior as chains without slip-springs. In contrast, longer chains ($N \geq 40 \approx 8\ N_e$) with slip-springs show a qualitatively different motion pattern with a deceleration of monomer motion, indicated by a negative slope in Figure 2. This retardation manifests itself in the famous $t^{1/4}$ regime (horizontal regime in Figure 3) where the motion perpendicular to the chain contour is restricted by the tube while the parallel motion is free. The onset of the entanglement effect occurs at about 4000 DPD timesteps. We demonstrate this confinement by calculating the correlation between the motion of the center of mass and the end-to-end vector of the chain. The time-dependent coefficient of the anisotropy $A_{cm}(t)$ has been defined by Likhtman[20] as

$$A_{cm}(t) = \frac{1}{2}\left(3\left\langle\left(\frac{(\vec{R}_{ee}(t) - \vec{R}_{ee}(0)) \cdot (\vec{r}_{cm}(t) - \vec{r}_{cm}(0))}{|\vec{R}_{ee}(t) - \vec{R}_{ee}(0)| \cdot |\vec{r}_{cm}(t) - \vec{r}_{cm}(0)|}\right)^2\right\rangle - 1\right), \quad (6)$$

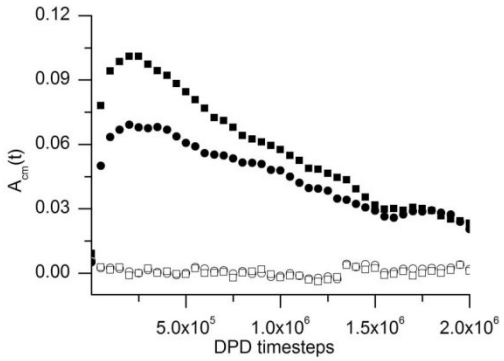

FIG. 4. Anisotropy coefficient $A_{cm}(t)$ for chains without (empty symbols) and with slip-springs (filled symbols). The chain length $N = 100$ is considered either completely (circles) or without the last 20 beads at both chain ends (squares).

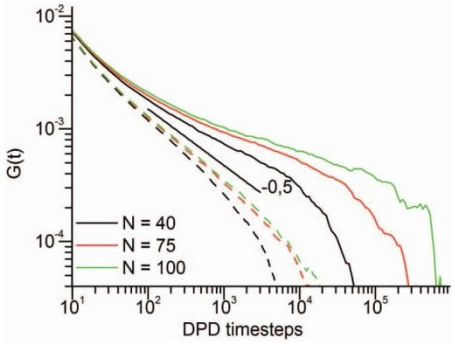

FIG. 5. Zero shear relaxation modulus $G(t)$ for chains without (dashed curves) and with slip-springs (solid curves). The chain length N ranges from 40 to 100. The straight line is a guide to the eye and demonstrates the Rouse scaling with $t^{-1/2}$.

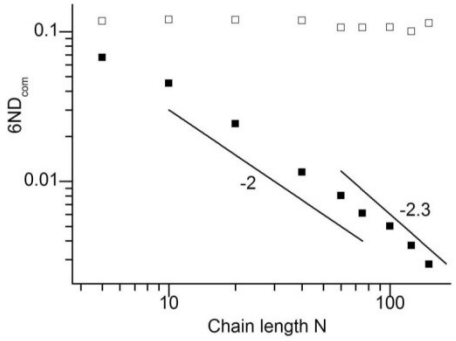

FIG. 7. Diffusion coefficient of the center of mass D_{com} scaled by $6N$ as a function of chain length for chains without (empty symbols) and with slip-springs (filled symbols). The two lines are guides to the eye and demonstrate the diffusion power law for reptation dynamics (-2) and the experimentally observed scaling behavior (-2.3).

where $\overrightarrow{R_{ee}}(t)$ is the end-to-end vector and $\overrightarrow{r_{cm}}(t)$ the position of the center of mass at time t. Figure 4 shows $A_{cm}(t)$ for chains of length $N = 100$ without (empty symbols) and with slip-springs (filled symbols). Moreover, the plot discriminates between two different ways to calculate $A_{cm}(t)$. For the circled curves, the whole chain (monomers 1 and 100) is considered. In the curves symbolized by squares, we take into account only the inner part of the chain (monomers 21–80) to attenuate possible chain-end effects. The motion of the center of mass is completely uncorrelated to the direction of the end-to-end vector for chains without slip-springs, whereas a small anisotropy for chains with slip-springs is clearly visible. Furthermore, as chain ends are less confined, the maximum of $A_{cm}(t)$ becomes higher if the chain ends are excluded. Slip-springs successfully hinder motion perpendicular to the chain contour. The overall dynamics is retarded and becomes less efficient in reducing stress or chain orientation due to its anisotropy of motion.

Figure 5 shows the shear relaxation modulus $G(t)$ calculated from the stress autocorrelation function.[21] In this specific study, we calculate the stress from all pair interactions not relying on the stress-optical law. For noise reduction, we applied the multi-tau correlator algorithm.[22] Chains without slip-springs (dashed curves) show Rouse relaxation with a slope of -0.5, whereas chains with slip-springs (solid curves) have a clear inflection. At this point, the negative slope increases towards zero and thus to the expected plateau, without actually reaching it for the chain lengths studied here. In Figure 6, $G(t)t^{0.5}$ amplifies variance of the Rouse behavior as deviations from the horizontal line.

Figure 7 exhibits the diffusion coefficient scaled by $6N$ as a function of N of chains without (empty symbols) and with (filled symbols) slip-springs. The chains without slip-springs obey Rouse dynamics with a power-law exponent of -1 for all chain lengths. In contrast, chains connected with slip-springs undergo a crossover in D that occurs at about $N_c = 2N_e$.[5] The chain lengths considered are not short enough to cover the whole crossover regime, and hence only the onset of the reptation dynamics can be seen. Then, diffusion decreases much faster with an exponent of -2 as predicted by reptation theory. The longest relaxation time τ_{rot} scaled by N^{-2}, shown in Figure 8, provides also an explicit impression on the retardation of the dynamics. The entanglements increase the power-law exponent from 2 to 3. The values of τ_{rot} are consistent with the horizontal regime in Figure 2 that corresponds to the disengagement time τ_d.

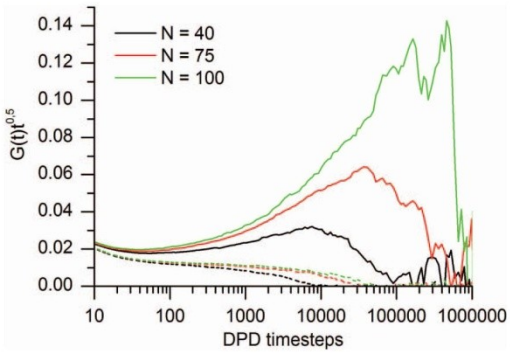

FIG. 6. Zero shear relaxation modulus $G(t)$ for chains without (dashed curves) and with slip-springs (solid curves) multiplied by $t^{1/2}$ to point out Rouse behavior as horizontal line. The chain length N ranges from 40 to 100.

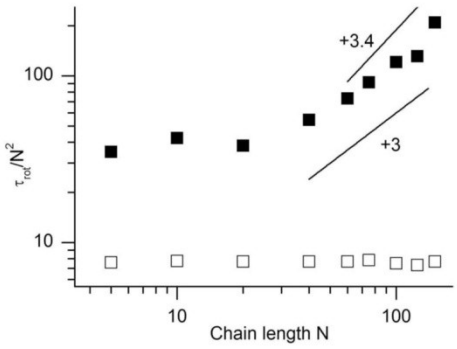

FIG. 8. Rotational relaxation time τ_{rot} scaled by N^{-2} against the chain length N for chains without (filled symbols) and with slip-springs (empty symbols). The two lines are guides to the eye and show the power 3 scaling law for reptation dynamics and power 3.4 scaling behavior observed from experiments.

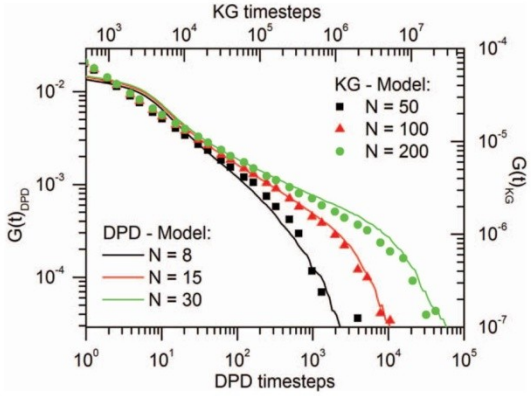

FIG. 9. Relaxation modulus $G(t)$ in comparison with KG simulations to evaluate computational efficiency of the DPD slip-spring model. The KG chains are shown by symbols and their length $N = 50$, 100 and 200 from left to right. The DPD slip-spring chains are shown by solid curves with the length $N = 8$, 15, and 30 from left to right.

Computational efficiency

The gain in computational speed in the present DPD approach relative to other competing models was done using the KG model as an effective standard. The reason for this is that the KG model is well established and treats entanglements naturally by excluded volume effects. Moreover, the computational efficiency of other approaches has been measured in comparison to the KG model, too. For instance, Slizoberg *et al.*[23] reported for the mSRP polymer model that similar entangled chains require half the number of particles and relax four times faster than simulated with the KG model. The multi-chain slip-spring model of Uneyama and Masubuchi[9] requires only one third the number of particles and the chains relax 50 times faster.

The entanglement length N_e can be chosen freely in the present model. It is close to 5 beads as described in the Simulation details section. KG chains have a seven times larger entanglement length of $N_e = 35$.[5] Therefore, comparable entangled polymer chains require seven times fewer particles in our slip-spring DPD model. The KG simulations were executed using the LAMMPS software from Sandia National Laboratories.[24] A complete description of the model and the corresponding parameters can be found in Ref. 5. The relaxation modulus $G(t)$ for DPD chains of length $N = 8$, 15, and 30 (solid curves) and KG chains of length $N = 50$, 100, and 200 (symbols) is shown in Figure 9. The curves of both models match with the fitting parameters (KG timestep/DPD timestep) = 500 and $(G(t)_{DPD}/G(t)_{KG}) = 290$. We compare the number of timesteps to measure the gain in efficiency because we assume that basically both DPD and MD steps can be processed at similar speed. However, we want to emphasize that the timestep in the present DPD simulation is ten times larger than in a KG simulation.

CONCLUSIONS

We have proposed an efficient way to mimic the entanglement effect in coarse-grained simulations using a slip-spring model. The implementation into a classical DPD formalism is straightforward and barely affects the computational speed. We have shown that the regular structure of DPD chains is not destroyed by the introduction of the slip-springs, even though we do not make use of any correction potential. This is, next to the constant number of slip-springs, another important simplification compared to Ref. 8. The analysis of the mean square displacement of the central bead reveals a retardation of monomer motion in the same way as proposed in the reptation model[2,3] and verified by traditional molecular dynamics.[5,25–27] The overall diffusion of the center of mass and the end-to-end vector decorrelation are decelerated, too, and obey the power law from reptation theory. Additionally, we demonstrate that the motion of the center of mass of a chain preferentially occurs in the direction of its end-to-end vector. This motional anisotropy leads to longer relaxation times for stress and chain orientation and is the cause for the plateau region of the zero shear relaxation modulus. Therefore, we may conclude that our slip-spring model constrains the chain monomers in a very similar manner as postulated in reptation theory. The scaling behavior proposed by reptation theory slightly deviates from experimental observations. It was found that the diffusion coefficient of the center of mass D scales with $t^{-2.3}$ instead of t^{-2} and that the rotational relaxation time τ_{rot} scales with $t^{3.4}$ instead of t^3.[28] It is commonly accepted that these deviations are due to some additional relaxation processes that are not considered in reptation theory, namely, contour length fluctuation and constraint release.[29] The hopping mechanism of this slip-spring model takes into account both relaxation processes. However, it is not the intention of the present work to determine the exact scaling behavior with a high precision. Though, it can be seen from Figures 7 and 8 that the scaling exponent gets close to the experimental value with longer chain lengths.

The present formalism uses a few parameters such as the number of steps of a DPD or MC sequence (n_{DPD} and n_{MC}), which cannot be chosen freely. The influence of these parameters on the overall statistical or dynamical properties is not yet completely understood. However, we noticed that the hopping mechanism must satisfy the detailed balance condition. Otherwise the polymer chains would start to collapse. Chappa *et al.*[8] also reported chain contraction in the absence of a correction potential. However, this behavior was only noticed for very small densities and the reason might be different to our observation. The number of steps n_{MC} for each MC sequence must be sufficiently large to ensure a certain mobility of the slip-springs. Furthermore, the rate of slip-spring relocations has an influence on the short-time mean square displacement and the onset of the entanglement effect (see the Appendix for a more thorough discussion concerning the impact of other n_{DPD} and n_{MC} values on the dynamics). Therefore, care must be taken to choose an appropriate number of DPD and MC steps per sequence in order to avoid an unphysical behavior. Moreover, the present model has an advantage over similar approaches[7,9,23] due to the multi-chain description and the use of DPD, specifically for possible applications where inter-molecular interactions and their diversity have significant effects. Polymer blends, copolymers, and composites are important examples of such systems. Finally, we would like

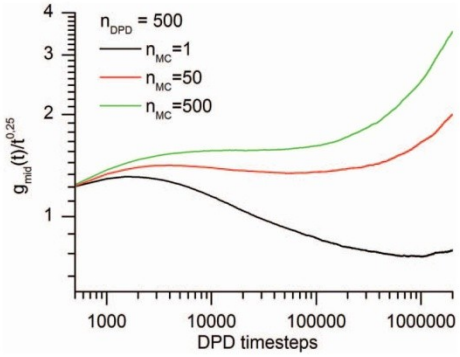

FIG. 10. Mean square displacement of the central bead $g_{1,mid}(t)$ scaled by $t^{1/4}$ for systems with different MC sequence lengths. The DPD sequence length is same for all systems, i.e., $n_{DPD} = 500$. Hereby, $n_{MC} = 500$ is the system on which the dynamical analysis from the Results section was carried out.

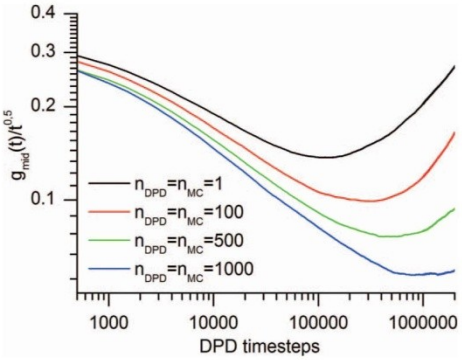

FIG. 12. Mean square displacement of the central bead $g_{1,mid}(t)$ scaled by $t^{1/2}$ to amplify the onset of the disengagement time τ_d for systems with different DPD and MC sequence lengths. The ratio n_{DPD}/n_{MC} is unity for all systems. Hereby, $n_{DPD} = n_{MC} = 500$ refers to the system on which the dynamical analysis from the Results section was carried out.

to point out that our approach is more efficient than a conventional molecular dynamics simulation with hard-core potentials to avoid chain crossings. According to our estimate, chains in the present DPD model contain 7 times fewer beads and the simulation is 500 times faster than in an equivalent molecular dynamics (KG)[5] model. Therefore, the apparent detour of first removing non-crossability by changing to a soft-core potential and then effectively re-introducing it via slip-springs does actually speed up the simulation.

ACKNOWLEDGMENTS

The present work has been supported by the Deutsche Forschungsgemeinschaft (DFG) within the priority program SPP1369.

APPENDIX: SEQUENCE LENGTHS

The impact of the choice of n_{DPD} or n_{MC} and their ratio on the chain dynamics is very interesting. In this appendix, we will examine the scaling behavior of the central bead mean square displacement $g_{1,mid}(t)$ with sequence lengths different from the ones used so far. However, we limit our discussion to only a single chain length of $N = 100$. At first, we will show the influence of decreasing n_{MC} at constant n_{DPD}, i.e., $n_{DPD} = 500$. As it was mentioned before, one would expect that the polymer melt turns into an elastomeric network when n_{MC} is reduced to zero. This assumption is confirmed by Figure 10 where n_{MC} has been reduced from its original value of 500 to 50 and 1 while n_{DPD} has a fixed length of 500 steps. The plot shows the onset of the famous $t^{0.25}$ scaling where the chain feels the constraints imposed by the tube. However, this regime is best reproduced for the system with $n_{MC} = 500$. The scaling exponent for the other two systems with decreasing n_{MC} has become smaller and is almost zero for the border case of $n_{MC} = 1$.

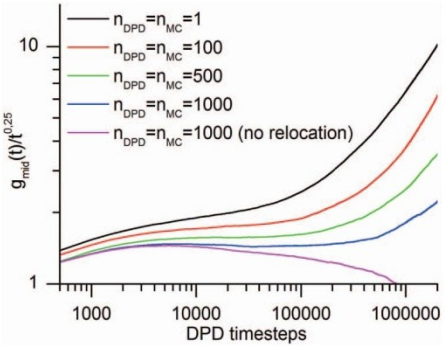

FIG. 11. Mean square displacement of the central bead $g_{1,mid}(t)$ scaled by $t^{1/4}$ for systems with different DPD and MC sequence lengths. The ratio n_{DPD}/n_{MC} is unity for all systems. Hereby, $n_{DPD} = n_{MC} = 500$ refers to the system on which the dynamical analysis from the Results section was carried out.

The system with $n_{DPD}/n_{MC} = 1$ provides the best results. Next, we discuss $g_{1,mid}(t)/t^{1/4}$ for different numbers of steps per sequence but keep the ratio $n_{DPD}/n_{MC} = 1$. Simulations with $n_{DPD} = n_{MC} = 1000$, 500, 100, and 1 have been carried out for this purpose. The relocation of slip-springs always takes place after a DPD sequence has finished and before a new MC sequence has begun. Therefore, the rate of relocations is raised with decreasing n_{DPD} and n_{MC}. Figure 11 illustrates that the $t^{1/4}$ regime is best achieved for the two systems $n_{DPD} = n_{MC} = 500$ and 1000. Though, the scaling exponent is much higher in the case of higher relocation rates, i.e., $n_{DPD} = n_{MC} = 1$ and 100. A possible explanation for this behavior might be that the disengagement time τ_d is reduced with increased relocation rate because the chains can quickly escape from their original confining environment. Therefore, the early onset of the free diffusion might interfere with the $t^{1/4}$ regime causing the scaling exponent to be slightly higher. This shift of τ_d to earlier times is amplified in Figure 12, where $g_{1,mid}(t)$ is scaled by $t^{1/2}$. Additionally, the border case with $n_{DPD} = n_{MC} = 1000$ but without relocation step in between a DPD and a MC sequence is shown in Figure 11, too. In this system, the chains do not have the ability to escape from their surrounding polymer chains to which they were initially connected by slip-springs. Thus, the central bead of a chain is caged and can only diffuse within a certain distance.

[1]P. E. Rouse, J. Chem. Phys. **21**, 1272 (1953).
[2]M. Doi and S. F. Edwards, *The Theory of Polymer Dynamics* (Clarendon, Oxford, 1986).
[3]P. G. de Gennes, J. Chem. Phys. **55**, 572 (1971).
[4]F. Müller-Plathe, ChemPhysChem **3**, 754 (2002).
[5]K. Kremer and G. S. Grest, J. Chem. Phys. **92**, 5057 (1990).
[6]N. A. Spenley, Europhys. Lett. **49**, 534 (2000).
[7]A. E. Likhtman, Macromolecules **38**, 6128 (2005).
[8]V. C. Chappa, D. C. Morse, A. Zippelius, and M. Müller, Phys. Rev. Lett. **109**, 148302 (2012).
[9]T. Uneyama and Y. Masubuchi, J. Chem. Phys. **137**, 154902 (2012).
[10]J. T. Padding and W. J. Briels, J. Chem. Phys. **115**, 2846 (2001).
[11]Y. Masubuchi, J.-I. Takimoto, K. Koyama, G. Ianniruberto, G. Marrucci, and F. Greco, J. Chem. Phys. **115**, 4387 (2001).
[12]D. Frenkel and B. Smith, *Understanding Molecular Simulation* (Academic, London, 2002).
[13]P. J. Hoogerbrugge and J. M. V. A. Koelman, Europhys. Lett. **19**, 155 (1992).
[14]G. Pan and C. W. Manke, Int. J. Mod. Phys. B **17**, 231 (2003).
[15]F. Goujon, P. Malfreyt, and D. J. Tildesley, J. Chem. Phys. **129**, 034902 (2008).
[16]T. W. Sirk, Y. R. Slizoberg, J. K. Brennan, M. Lisal, and J. W. Andzelm, J. Chem. Phys. **136**, 134903 (2012).
[17]M. Yamanoi, O. Pozo, and J. M. Maia, J. Chem. Phys. **135**, 044904 (2011).
[18]P. Español and P. Warren, Europhys. Lett. **30**, 191 (1995).
[19]R. D. Groot and P. B. Warren, J. Chem. Phys. **107**, 4423 (1997).
[20]A. E. Likhtman, "Viscoelasticity and molecular rheology," *Polymer Science: A Comprehensive Reference* (Elsevier, Amsterdam, 2012), pp. 133–179.
[21]P. Kindt and W. J. Briels, J. Chem. Phys. **127**, 134901 (2007).
[22]D. Magatti and F. Ferri, Appl. Opt. **40**, 4011 (2001).
[23]Y. R. Slizoberg, T. W. Sirk, J. K. Brennan, and J. W. Andzelm, J. Polym. Sci., Part B: Polym. Phys. **50**, 1694 (2012).
[24]S. Plimpton, J. Comput. Phys. **117**, 1 (1995).
[25]A. E. Likhtman, S. K. Sukumaran, and J. Ramirez, Macromolecules **40**, 6748 (2007).
[26]A. Rakshit and R. C. Picu, J. Chem. Phys. **125**, 164907 (2006).
[27]Q. Sun and R. Faller, Macromolecules **39**, 812 (2006).
[28]T. P. Lodge, Phys. Rev. Lett. **83**, 3218 (1999).
[29]C.-Y. Liu, R. Keunings, and C. Bailly, Phys. Rev. Lett. **97**, 246001 (2006).

THE JOURNAL OF CHEMICAL PHYSICS **141**, 194904 (2014)

Reptation and constraint release dynamics in bidisperse polymer melts

Michael Langeloth,[1,a)] Yuichi Masubuchi,[2] Michael C. Böhm,[1] and Florian Müller-Plathe[1]
[1]*Eduard-Zintl-Institut für Anorganische und Physikalische Chemie and Center of Smart Interfaces, Technische Universität Darmstadt, Alarich-Weiss-Straße 4, D-64287 Darmstadt, Germany*
[2]*Institute for Chemical Research, Kyoto University, Gokasho, Uji 611-0011, Japan*

(Received 9 July 2014; accepted 29 October 2014; published online 17 November 2014)

Bidisperse melts of linear, entangled polymer chains were studied using dissipative particle dynamics. The entanglement constraints were mimicked with our newly developed slip-spring approach. The compositions cover blends with short matrix chains, slightly above the molecular entanglement weight as well as blends were both chain lengths exhibit distinct entangled dynamics at various weight fractions. The Struglinsky-Graessley parameter Gr, which is the ratio between the relaxation time of the long chains due to pure reptation and the relaxation time of the tube caused by constraint release, ranges between values high above and below unity. We compare our slip-spring model with simulations that use conventional generic polymer models where bond crossings are prevented by excluded-volume interactions and find fairly good agreement in terms of the mean squared displacement. However, the slip-spring approach requires only a fraction of the computational time, making large scale systems feasible. The dynamical interference of the two different chain lengths is discussed in terms of reptation and constraint release dynamics. For bidisperse melt compositions with $Gr < 1.0$ the relaxation time of the long chain component is not affected by constraint release. However, for compositions where constraint release is supposed to contribute significantly to the relaxation mechanism ($Gr > 1.0$), we find strong evidence that the long chains reptate inside a dilated tube whose diameter increases with an exponent of 1/2 towards lower weight fraction of the long chains. Furthermore we observe a linear relation between the relaxation time and weight fraction. Therefore, based on the relaxation times, our results support the validity of the tube dilation model as proposed by Doi *et al.* [Macromolecules **20**, 1900–1906 (1987)]. © *2014 AIP Publishing LLC*. [http://dx.doi.org/10.1063/1.4901425]

I. INTRODUCTION

The reptation model describes successfully the dynamics of entangled, monodisperse polymer chains.[1] Entanglements are only of relevance for chains exceeding the entanglement molecular weight M_e, i.e., the average molecular weight between two entanglements. In contrast to the faster Rouse dynamics, which applies to all chain lengths below the threshold M_e, reptation dynamics confines the chain within a "tube" imposed by the neighboring chains. The individual monomers do not realize this confinement immediately. At first, the mean square displacement of the central chain bead $g_1(t)$ follows the Rouse scaling $g_1(t) \propto t^{0.5}$. This behavior changes at the entanglement time τ_e when the chain beads reach the tube diameter a. From this point, $g_1(t)$ continues with a smaller time exponent of only 0.25. In the concept of reptation,[2] the chain crawls out of the tube along the contour line like a slithering snake. This subdiffusive regime lasts until the Rouse time τ_R where the time exponent changes back to 0.5. The free diffusive regime begins at the time τ_d when the chain has left the tube. Additionally, it is known that processes other than pure reptation, namely contour-length fluctuations[3] and constraint release[4] play an important role for the viscoelastic behavior. They must be incorporated to obtain qualitative agreement with experimental studies on viscosity or diffusion.[5] Contour-length fluctuation is a single-chain effect that arises from stretching and contracting of the chain within the confining tube. It effectively reduces the life time of a tube τ_d and, hence, decreases the reptation time compared to pure reptation.[3,6]

Constraint release, on the other hand, is a multi-chain effect and becomes most important in polydisperse polymers. The tube model[1] says that, for monodisperse melts, the lifetime of an obstacle that confines a chain inside a tube is as long as the relaxation time of the surrounding chains. In polydisperse systems the situation changes. The lifetime of an entanglement now depends additionally on the chain lengths involved. Entanglements between short and long chains dissolve quickly owing to the fast relaxation of the short chains.[7] As a consequence, a long chain may leave its confining tube also in a direction perpendicular to its contour line.[4,8] This constraint release allows the long chains to relax more quickly than by a pure reptation process.[7] The Struglinski-Graessley parameter (Eq. (1)) is useful in means of quantifying the influence of constraint release mechanisms on the relaxation time. It is defined as

$$Gr = M_l M_e^2 / M_s^3, \tag{1}$$

where M_l and M_s are the molecular weight of the long and short chains and M_e the entanglement molecular weight. It can be understood as the ratio between the relaxation time of

a)Author to whom correspondence should be addressed. Electronic mail: m.langeloth@theo.chemie.tu-darmstadt.de

the long chains due to pure reptation and the relaxation time of the tube caused by constraint release.

The two most prominent theoretical approaches for bidisperse polymer systems are the tube dilation model of Doi *et al.* and of Marrucci[7,8] as well as the tube reptation model of Viovy *et al.*[9] These authors all draw the same conclusions for melts with *Gr* smaller than unity and agree that the chains reptate inside an undilated tube.[7–9] The mean square displacement $g_1(t)$ does not only consist of a contribution of the pure reptation mechanisms $g_{rep}(t)$ but is additionally accelerated by the tube Rouse motion $g_{tube}(t)$ (Eq. (2)).[4] However, τ_d is hardly affected because the relaxation time of pure reptation $\tau_{d,rep}$ is much shorter than the relaxation time of the tube Rouse motion $\tau_{d,tube}$ (Eq. (3)),

$$g_1(t) = g_{rep}(t) + g_{tube}(t), \tag{2}$$

$$1/\tau_d = 1/\tau_{d,rep} + 1/\tau_{d,tube}. \tag{3}$$

For melts with *Gr* larger than unity the relaxation process is governed by constraint release mechanisms. In this regime, the two theories of Doi *et al.*[7] and Viovy *et al.*[9] differ conceptually and come to very different conclusions. Doi *et al.* predict that the chain reptates inside a dilated tube.[7] Viovy *et al.* treat the tube diameter as a constant and imagine that the tube itself reptates inside a second, larger tube which is often referred to as "supertube".[9] According to Doi's tube dilation model the relaxation time increases linearly with the concentration of the long chains until it reaches the reptation time of the pure long-chain melt at $\phi_l = 1.0$,[7]

$$\tau_d \sim \phi_l \quad \text{for}: 1/Gr \le \phi_l \le 1. \tag{4}$$

In contrast to this, Viovy *et al.* predict that the relaxation time increases linearly until it reaches the "chain reptation" regime, after which it remains independent of ϕ_l,[9]

$$\tau_d \sim \phi_l \quad \text{for}: \quad M_e/M_l \le \phi_l \le \left(M_e/M_s\right)^3, \tag{5}$$

$$\tau_d = const. \quad \text{for}: \left(M_e/M_s\right)^3 \le \phi_l \le 1.0. \tag{6}$$

Despite their industrial importance, relaxation processes of polymer melts with two or more different chain lengths have not yet been thoroughly addressed in molecular dynamics simulations. This is probably related to the large length and time scales which make the simulations very time consuming. However, the need for a deeper understanding of the relaxation mechanisms emerges from the fact that polydisperse polymer melts are the rule rather than the exception in real polymeric processing and materials. As a result, the enhanced relaxation by constraint release is not only interesting from a theoretical view point. Furthermore, since the relaxation time determines the rheological behavior, it plays a crucial role in the development and design of new materials.

There have been only a few molecular simulations of binary mixtures with small and large molecular weights M_s and M_l.[10,11] Wang and Larson[11] performed simulations of bidisperse mixtures using a generic polymer model[12] that prevents bond-crossings by excluded-volume interactions. They reported that constraint release effects become prominent right after the entanglement time τ_e, although all theoretical models[7–9] assume that this process is negligible before the disentanglement of the short chains.[11] This discrepancy is said to be mostly caused by contour-length fluctuations and crossover effects of various time regimes.[11] It is anticipated that simulating longer chain lengths would reduce these disagreements with theory. This is, however, not feasible with the computational power available.[11] Dissipative particle dynamics (DPD) is fast compared with standard molecular dynamics and was developed for the simulation of mesoscale liquids.[13] Its thermostat conserves momentum locally, and hence reproduces the correct hydrodynamic behavior. The inter-bead potentials are too soft to prevent chain crossings so that polymer chains in DPD simulations usually show no sign of entanglement.[14] However, there have been some attempts in the past, which try to restore entangled polymer dynamics to DPD or Brownian dynamics simulations.

One rigorous approach is to introduce uncrossability between chains by the segmental repulsive potential[15] or by the TWENTANGLEMENT approach.[16] Another, conceptually very different approach is the insertion of temporary bonds (slip-springs) that migrate along the chains and which successfully mimic entangled behavior in DPD.[17] Both approaches are expected to capture the constraint-release effect as they model the interaction of multiple chains. However, the artificial implementation of entanglement constraints of the second approach requires additional tests of the reproduction of entanglement dynamics, as it has been done for the slip-link simulations.[18,19] Therefore, this paper will first compare the diffusive behavior of our slip-spring model with results of a Kremer-Grest simulation.[11] After that we expand the bidisperse systems to larger molecular weights and compare the relaxation mechanism for melts with *Gr* below and above unity to distinguish between the existing theoretical models[7–9] and to verify their validity.

II. METHOD

In the present study we simulate systems of long chain lengths by using a parallelized version of our newly developed multi-chain slip-spring model.[17] Dissipative particle dynamics (DPD) is employed to simulate the motion of the chains, each DPD bead representing several chemical repeat units.[20] The reduced number of degrees of freedom makes the computation faster and the smaller friction in the system accelerates the bead dynamics. As there is no hard-core repulsion in the nonbonded DPD potential,[13] however, polymer chains can cross each other. Consequently, the dynamics of a polymer melt in DPD simulations is always Rouse-like, regardless of the molecular weight.[14,15] In our previous study[17] we have shown that the entangled dynamics can be restored to DPD simulations with the help of slip-springs which mimic entanglements as binary events. They are modeled by a harmonic potential with the same spring constant as chain bonds and are placed between beads of two different chains and also between distant beads of the same chain. Slip-springs can migrate along the chain. Once a slip-spring has reached a chain end it may relocate to another randomly selected chain end. All slip-spring motion is controlled by the Metropolis Monte

Carlo algorithm ensuring detailed balance.[21] A detailed description of the slip-spring method is provided in Ref. 17. The apparent detour of first removing entanglements by using a higher coarse grained model and second reinserting the entanglement effect by artificial slip-springs actually speeds up the computation greatly. Our previous study estimates a gain in CPU time by two orders of magnitude compared to standard molecular dynamics with hard-core bead-bead interactions.[17] We also want to draw the reader's attention to the work of Chappa *et al.*,[22] Uneyama and Masubuchi[23] as well as Ramírez-Hernández *et al.*[24] who pursued similar approaches using multi-chain slip-spring models. In particular, Ramírez-Hernández *et al.*[24] demonstrated good agreement of the loss and storage moduli for mono- and bidisperse polystyrene melts with experimental values.

We work in reduced units and scale energy, monomer mass and the cutoff length to unity, hence, $k_BT = m = r_c = 1$. The nonbonded-interaction is purely repulsive with a force that decays linearly with the distance r_{ij} between beads i and j, i.e., $\vec{F}_{ij} = a_{ij}(1 - \vec{r}_{ij}/r_c)$ with a repulsion parameter $a_{ij} = 25k_BT/r_c$. Neighboring beads along a chain are harmonically coupled with a spring constant of $2k_BT/r_c^2$. The same potential has been used to model slip-spring interactions. The integration is performed with a time step of $\Delta t = 0.06\tau$, where τ is the time unit $\tau = mr_c^2/k_BT$. The temperature is maintained using the DPD thermostat with a noise amplitude of $\sigma = 3$ and, according to the fluctuation dissipation theorem,[25] a friction parameter of $\gamma = 4.5$. The length of the cubic box is $l = 24r_c$ for all systems. The composition of the binary melt can be described by two parameters Gr and ϕ_l. The weight fraction of the long chains in the system, ϕ_l is defined as $\phi_l = M_l n_l/(M_s n_s + M_l n_l)$ with n_s, M_s and n_l, M_l the numbers and molecular weights of the short and long chains, respectively. Throughout we will use a subscript s when referring to properties regarding short chains and l for the long chains.

TABLE I. Summary of polymer melt compositions: n_s and n_l are the numbers of short and long chains with molecular weights M_s and M_l, respectively. The weight fraction is defined as $\phi_l = M_l n_l/(M_s n_s + M_l n_l)$. The Struglinski-Graessley parameter Gr was calculated using $M_e = 5.5$. The density ρ in reduced units is given in the last column.

System (M_s/ϕ_l)	$n_l \times M_l$	$n_s \times M_s$	Gr	$\rho(r_c^{-3})$
04/015	31 × 56	2503 × 4	26.5	0.85
08/015	31 × 56	1251 × 8	3.31	0.85
13/015	31 × 56	770 × 13	0.25	0.85
26/015	31 × 56	385 × 26	0.096	0.85
56/100	210 × 56	...	0.0096	0.85
010/015	21 × 300	3510 × 10	9.1	3.00
050/015	21 × 300	702 × 50	0.07	3.00
100/015	21 × 300	351 × 100	0.009	3.00
010/030	41 × 300	2910 × 10	9.1	3.00
010/060	83 × 300	1650 × 10	9.1	3.00
010/070	97 × 300	1230 × 10	9.1	3.00
010/080	110 × 300	840 × 10	9.1	3.00
010/090	124 × 300	420 × 10	9.1	3.00
300/100	138 × 300	...	0.0003	3.00

Table I summarizes the composition of the various melts discussed here. Our notation for these systems contains the short chain molecular weight M_s and the long chain weight fraction ϕ_l, separated by a slash. Except for the first five low-density systems, we use a density of $\rho = 3r_c^{-3}$ as we did in our previous study.[17] All polymer melts were first equilibrated without slip-springs to benefit from the faster Rouse dynamics. After equilibration, we inserted 1175 slip-springs for the low-density melts and 4140 for the other systems with higher density including the monodisperse system. The number of slip-springs is a parameter which controls the average distance along the chain between two slip-springs and hence the total number of slip-springs per chain. It can be chosen freely between two limits. First, the subchains between two slip-spring points should be long enough to allow Rouse relaxation. Second, the number of slip-springs should be sufficiently large to observe distinct entangled behavior. In our previous work[17] we have chosen one slip-spring per ten beads, such that every fifth bead is connected by a slip-spring. In the present study, we keep this ratio. Since slip-springs do not repel each other, two or more slip-springs may also temporarily connect the same bead. Therefore, the average length of a subchain between two slip-spring points becomes slightly larger than 5 beads, i.e., $M_e = 5.5$. For the largest chains in our systems with $M_l = 300$ we get an average value of $Z = M_l/M_e \approx 55$ slip-springs per chain.

III. RESULTS AND DISCUSSION

A. Comparison with the Kremer-Grest model

The first five compositions in Table I have a Gr parameter that ranges from 0.01 to 26.5. The weight fraction $\phi_l = 15\%$ is low enough to neglect constraints imposed by long-long entanglements. Figure 1 combines $g_{1,l}(t)$ of these DPD systems together with some data points of comparable Kremer-Grest (KG) molecular dynamics simulations from Wang and Larson.[11] The KG bead-spring model[12] prevents bond crossings explicitly by excluded volume interactions. The length of their long chains is $M_l = 350$. The precise value of the

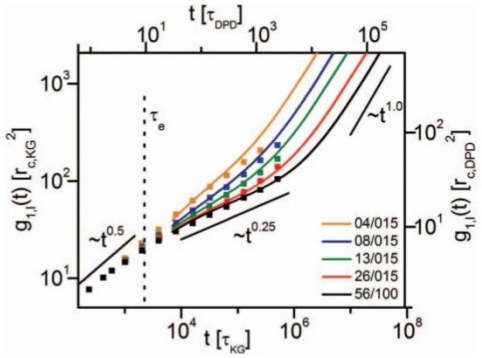

FIG. 1. The solid curves illustrate the mean square displacement $g_{1,l}(t)$ of the slip-spring systems (04-26)/015 and 56/100 (from top to bottom). The Struglinsky-Graessley parameter Gr ranges from 26.5 for system 04/015 to 0.0096 for the monodisperse system 56/100. The filled symbols show $g_{1,l}(t)$ results from Wang and Larson using the Kremer-Grest model.[11] The dashed vertical line illustrates the transition from Rouse to repation scaling.

entanglement length for the Kremer-Grest chains is still an ongoing discussion and might depend on how M_e is measured. A consensus of M_e in the range of 23 to 35 Kremer-Grest beads seems to have been reached in the literature, but higher estimates exist as well.[26] We use the same mapping scheme ($6.6M_{KG} = 1\ M_{DPD}$) as in our previous publication.[17] Hence, the number of entanglements in Kremer-Grest chains is close to the number of slip-springs in our DPD simulation. This scaling may be crude, especially for short chains. Notwithstanding, the curves of both models match fairly well when scaling $\tau_{DPD} = 250\tau_{KG}$ and $r_{c,\,DPD} = 3.6r_{c,\,KG}$. Wang and Larson[11] estimated that τ_e, the transition time from Rouse to reptation scaling, occurs at $2290\tau_{KG}$. In agreement with their observation, we also find that the onset of constraint release effects occurs right after τ_e (dashed vertical line) and not after the disentanglement of the short chains. This finding is in contrast to theoretical models[7–9] and is probably due to crossover effects of various time regimes and contour-length fluctuations.[11] After τ_e, the curves continue with an exponent ranging from pure reptation for the monodisperse melt up to Rouse motion for the lowest M_s. It is evident that $\tau_{d,l}$ shifts to much earlier times when M_s is reduced. The figure also demonstrates the striking advantage of our slip-spring model in terms of efficiency. While the accessible time scale for Kremer-Grest chains of such systems is limited to about the disentanglement time, the slip-spring model easily reaches far into the free diffusive regime and allows us to measure the diffusion coefficients of the different systems.

The diffusion coefficients D_l of the long chains of systems (04-26)/015 together with those of the monodisperse system 56/100 can be seen in Figure 2 as filled circles. For better comparison with experimental data, D_l is normalized by $D_{l,mono}$, i.e., the diffusion coefficient of the long chains in the monodisperse system. Likewise, M_s is normalized by M_l. The diffusion coefficient D_l/D_{mono} against M_s/M_l scales with an exponent somewhat lower than -1. Similar observations have been made by Wang *et al.*[27] for polybutadiene chains of comparable length with $\phi_l = 20\%$ and 10%. Both cases are added to Figure 2 as open symbols.

Systems 050/015 and 100/015 in Table I have the same weight fraction $\phi_l = 15\%$ as the systems in Figure 1 but their molecular weights are considerably higher. For the two systems 050/015 and 100/015, both long and short chains are

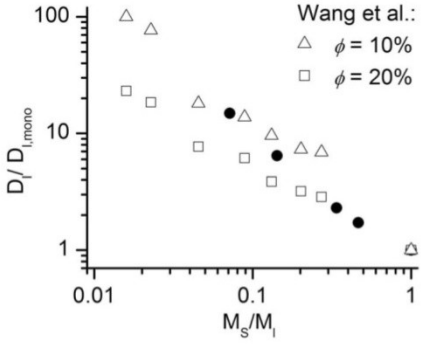

FIG. 2. $D_l/D_{l,mono}$ of the slip-spring systems (04-26)/015 and 56/100 against M_s/M_l (filled symbols). The open symbols show experimental results from Wang *et al.*[27]

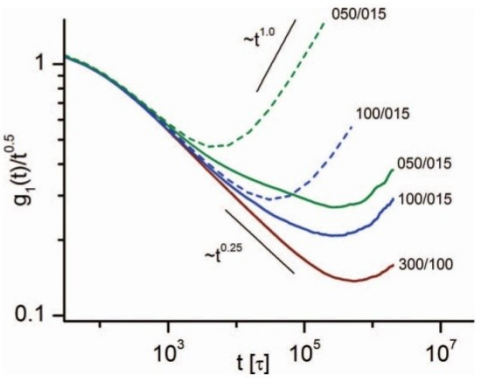

FIG. 3. Mean square displacement $g_1(t)/t^{0.5}$ of the short (dashed lines) and long (solid lines) chains of systems 050/015, 100/015, and 300/100. The scaling of $g_1(t)$ highlights the relaxation time of the chains. *Gr* is below unity for all three melt compositions.

well entangled and $\tau_{d,s}$ should differ markedly from τ_e or $\tau_{d,l}$. Thus, neither crossover effects between different time regimes nor strong contour-length fluctuations are expected. Figure 3 shows $g_{1,s}(t)$ (dashed curves) and $g_{1,l}(t)$ (solid curves) of systems 050/015, 100/015, and 300/100. The mean square displacement has been scaled by $t^{0.5}$ to highlight the relaxation time of the chains. The entanglement effect with its $t^{0.25}$ scaling is clearly visible for the long and short chains of systems 050/015 and 100/015. However, the reptation regime of the long chains is much shorter in the binary mixture than in the monodisperse melt. We observe a change to higher exponents that lie between the reptation and Rouse scaling (i.e., $t^{0.5}$, which would be horizontal line in the scaling of Fig. 3). This upturn happens right after the relaxation of the short chain matrix. For $t < \tau_{d,s}$, though, the behavior of binary and monodisperse melts is indistinguishable. This upturn of $g_1(t)$ has been predicted by Marrucci, Doi *et al.*, and Viovy *et al.*[7–9] They all assume that for a melt with $Gr < 1$, the long chain reptates in an undilated tube. Then, at the relaxation time of the short chains $\tau_{d,s}$, constraint release effects become prominent and lead to a Rouse-like motion of the tube. After that time the short chain matrix can be regarded as solvent which does not contribute to the confinement of the long chains anymore. Thus $g_{1,l}$(t) increases by the contribution of the tube motion (Eq. (2)). The relaxation time of the long chains, however, is dominated by the faster chain reptation and thus, is hardly affected by M_s or ϕ_l (Eq. (3)).

B. Tube dilation

The theoretical models predict a different behavior for $Gr > 1$. Marrucci and Doi *et al.*[7,8] propose "restricted tube dilation" for $\phi_l > 1/Gr$. At higher weight fractions the number of long-long entanglements is high enough to restrict the long chains within a tube even after the relaxation of the short chains. The decline of entanglements causes the dilated tube diameter for the long chains to increase to a certain extent. For $\phi_l < 1/Gr$; however, the number of remaining long-long entanglements is not sufficient anymore. Consequently, the tube diameter can grow without limits and, thus, the process is called "free dilation." Systems 010/(015-090) have the same

molecular weight $M_s = 10$ but various weight fractions ranging from $\phi_l = 15\%$ to 90%. For such short chains we assume that they relax almost instantaneously. Moreover, the long chains will swell slightly since $M_l > M_s^2$.[28] However, this effect is insignificant for the present simulations and additionally superimposed by the fact that the pressure in our system changes with the number of attractive interactions, i.e., the number of chain bonds and slip-springs. Inevitably, the bond lengths are slightly stretched (less than 4%) for systems with lower weight fractions.

The determination of the dilated tube diameter a from computer simulations is a delicate issue as addressed by Likhtman *et al.*[29] Tube dilation theory predicts that a depends on ϕ_l according to $a = a_{mono}\phi_l^{-\alpha/2}$ where a_{mono} is the tube diameter for the monodisperse system and $\alpha = 4/3$. The precise value of α is a matter of debate. While some experiments and theories suggest $\alpha = 4/3$ others find better agreement with $\alpha = 1.0$.[30–33] Van Ruymbeke *et al.* discussed the value of the dilution exponent in their study and concluded that it varies from system to system depending on the tension equilibration process.[34] We emphasize that if the tube diameter is determined by the number of slip-springs between long chains, the exponent should be unity by construction. Thus, the exponent of 4/3 is owing to the local segmental motion as discussed by van Ruymbeke *et al.*[34] Once, Kremer and Grest[12] proposed to derive the tube diameter from the mean square displacement of the central bead. Here, one assumes that the long chains show a transition from Rouse-like behavior to reptation in $g_{1,l}(t)$. The value of $g_{1,l}(t)$ at the transition then corresponds to the squared (dilated) tube diameter. However, the discrimination between dilution exponents of $\alpha = 1.0$ and $\alpha = 4/3$ is quite challenging due to the rather broad transition in $g_{1,l}(t)$ which makes it difficult to localize the tube diameter. We, therefore, pursue a different approach based on primitive-path statistics (see Eq. (7)).[35] The squared end-to-end distance $\langle R_{ee}^2 \rangle$ and the primitive-path $\langle L_{pp} \rangle$ are exclusively referring to the long chains. $\langle L_{pp} \rangle$ is defined as the length from one chain end to another passing all beads that hold a long-long slip-spring. The angle brackets $\langle \dots \rangle$ indicate a time average over all long chains. Slip-springs that span over a long and a short chain are neglected as a result of the fast relaxation of the short chains. In this connection the tube diameter a can be interpreted as the Kuhn length of the tube,

$$a = \frac{\langle R_{ee}^2 \rangle}{\langle L_{pp} \rangle}. \tag{7}$$

Figure 4 displays the results from the primitive-path analysis in a double logarithmic scale showing the tube diameter a against the volume fraction ϕ_l for the systems 010/(060-090) and 300/100. The results agree fairly well to a tube dilation exponent of $\alpha = 1.0$ as indicated by the straight line. As described by Milner, this outcome is presumably owed to the fact that the primitive-path considers entanglements only as a binary event, neglecting that the tube formation is a result of contacts between nearby chains with each other, too.[36]

Figure 5 focuses on the transition region from Rouse to reptation dynamics. It shows $g_{1,l}(t)/t^{0.25}$ of systems 010/(015-090) and 300/100 (from top to bottom). The mean square displacement has been scaled by $t^{0.25}$ to highlight the onset of the reptation regime. The stars indicate the time after which $g_{1,l}(t)$ has reached the tube diameter. These values were obtained from the previous primitive-path analysis. The absence of a distinct transition point prevents a direct comparison of the tube diameter obtained from primitive-path analysis and $g_{1,l}(t)$ as proposed by Kremer and Grest.[12] Yet, the values appear to coincide very well with the onset of the reptation regime in $g_{1,l}(t)$. On the other hand, the long chains in systems 010/015 and 010/030 are not well constrained anymore. Though, for $\phi_l = 30\%$, the remaining long-long entanglements still have an impact on $g_{1,l}(t)$, causing a kink toward smaller exponents. This transition to "free dilation" is consistent with the theoretical prediction $\phi_l < 1/Gr$, even though our weight fraction is higher.

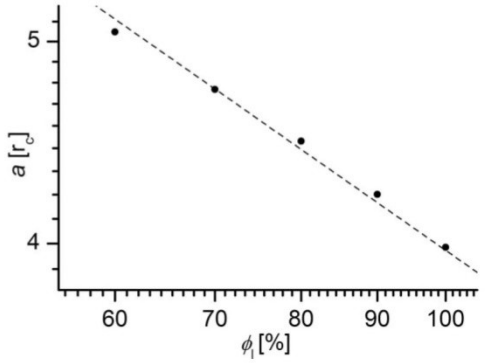

FIG. 4. Tube diameter against ϕ_l of systems 010/(060-090) and 300/100 in a double logarithmic plot. The dashed line emphasizes the proposed relation for restricted tube dilation $a = a_{mono}\phi_l^{-\alpha/2}$ with $\alpha = 1.0$.

C. Relaxation time

The analysis of $\tau_{d,l}$ provides deeper insight into the dominant relaxation process. The theories of Doi *et al.*[7] and Viovy *et al.*[9] assume different conceptional views of the underlying mechanism and lead to qualitatively different assertions.

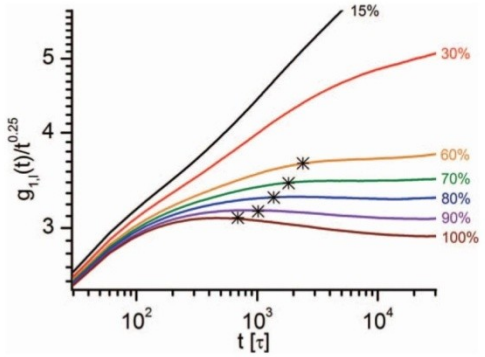

FIG. 5. Mean square displacement $g_{1,l}(t)/t^{0.25}$ of systems 010/(015-090) and 300/100 (from top to bottom). The stars indicate the time when $g_{1,l}(t)$ has reached the tube diameter a derived from primitive-path analysis. The mean-square displacement has been scaled to emphasise the reptation regime, which can be recognised by a horizontal curve. The Struglinsky-Graessley parameter Gr is for all bidisperse systems above unity.

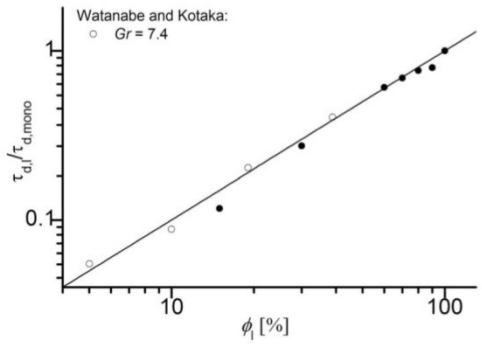

FIG. 6. Normalized relaxation time $\tau_{d,l}/\tau_{d,mono}$ against ϕ_l for the systems 010/(015-090) and 300/100. The line illustrates linear behaviour. The open symbols show experimental results of Watanabe and Kotaka.[37]

Viovy *et al.* argue that $\tau_{d,l} \propto \phi_l$ in the range of $M_e/M_l < \phi_l < (M_e/M_s)^3$ due to tube reptation inside a "supertube" (Eq. (5)). Pure chain reptation becomes the dominating relaxation mechanism for $\phi_l > (M_e/M_s)^3$ (Eq. (6)). From this it follows that $\tau_{d,l}$ becomes independent of ϕ_l and thus remains constant in the range $(M_e/M_s)^3 < \phi_l < 1$.[9] In sharp contrast to this, Doi *et al.* propose that $\tau_{d,l} \propto \phi_l$ in the range of $1/Gr < \phi_l < 1$ due to "restricted dilation" (Eq. (4)).[7] The results of the systems 010/(015-090) and 300/100 are shown in Figure 6. Here, $\tau_{d,l}$ has been derived from an exponential fit of the autocorrelation function $\Theta_l(t) = \langle \vec{R}_{ee,l}(t) \cdot \vec{R}_{ee,l}(0) \rangle$, where $\vec{R}_{ee,l}(t)$ is the end-to-end vector of the long chains. The time it takes until the chain orientation is no longer correlated corresponds to $\tau_{d,l}$, the time a chain needs to leave its tube. In the plot, $\tau_{d,l}$ is normalized by the relaxation time in the monodisperse case $\tau_{d,mono}$. The straight line is a guide to the eye and illustrates a power law of 1.0. Our results match this line fairly well and suggest a linear behavior as proposed by tube dilation theory.[7]

Figure 6 also displays experimental results of Watanabe and Kotaka[37] (i.e., system L1070/L36, equivalent to $Gr = 7.4$) with polystyrene chains of similar dispersity as used in our simulations. However, it appears that this scaling holds only for marginally entangled short chain lengths that are sufficiently close to M_e. The experimental studies of Watanabe and Kotaka[37] as well as Wang *et al.*[38] both show that the scaling exponent is not independent of M_s but decreases towards smaller values when M_s is significantly raised above M_e.

IV. CONCLUSION

In the current study we expanded our slip-spring model[17] to bidisperse polymer systems with two different chain lengths at various concentrations. The Struglinski-Graessley parameter Gr of those systems ranges from values above and below unity. Thereby, the described systems cover the two regimes where the relaxation time of the long chains is reduced by the constraint release mechanism ($Gr > 1$) and where the relaxation time is allegedly unaffected by the constraint release effects ($Gr < 1$).[7] The slip-spring model is very efficient compared to methods that prevent chain crossings by excluded volume potentials, e.g., the Kremer-Grest approach.[12] We estimate the gain in computational speed to be two orders of magnitude.[17] This facilitates simulations of longer time and length scales which are necessary in particular for systems with a low long-chain concentration ϕ_l or for systems with two very different chain lengths.

The slip-spring model qualitatively reproduces the diffusive behaviour of previously simulated Kremer-Grest polymer melts (Fig. 1).[11] The time scales accessible by the slip-spring model facilitate the observation of the free diffusive regime and allow a favourable comparison with the experimental diffusion coefficients of Wang *et al.*[27] (Fig. 2). For a content of 15% long chains, we find that the diffusion coefficient decreases almost linearly with increasing length of the short matrix chains. The experimental values for melts with $\phi_l = 10\%$ and $\phi_l = 20\%$ are just above and below our simulations.[27] Wang and Larson reported that for their Kremer-Grest simulations the constraint release effects occur immediately after the entanglement time τ_e.[11] This is in disagreement with existing theoretical models and probably due to contour length fluctuations and overlapping time regimes of the long and short chains.[7–9] We also observe this behaviour in our slip-spring simulation with comparable melt compositions (systems (04-26)/015 and 56/100); it, however, disappears for system with longer chain lengths (systems 050/015, 100/015, and 300/100).

Although we use a generic bead-spring polymer model, we assume that our findings can be applied qualitatively to real polymer systems as well. Therefore, we analyzed systems with more disparate chain lengths in different time regimes. The mean square displacement (Fig. 3) for polymer melts with a Struglinski-Graessley parameter $Gr < 1$ agrees with all theoretical predictions. The constraint release effects do not set in before the relaxation time of the short chains $\tau_{d,s}$. Furthermore, the long-chain relaxation time $\tau_{d,l}$ is not affected by the presence of the short chain matrix. For melts with $Gr > 1$ (Figs. 4 and 5) we observe a widening of the tube using primitive-path analysis.[35] The tube diameter a scales with the concentration of long chains as $a = a_{mono}\phi_l^{-\alpha/2}$ with a dilation exponent of $\alpha = 1.0$. Furthermore, we show (Fig. 6) that the relaxation time of the long chains scales linearly with ϕ_l even for concentrations close to the monodisperse limit. The later outcome favors the tube dilation theory[7,8] over tube reptation.[9] Consequently, rheological properties that depend on the relaxation time (e.g., the viscosity of a polymer melt) can be tailored to suit the material requirements with the addition of short chain lengths. However, the long and short chains must be of disparate length ($Gr > 1$) for the chains to disentangle more quickly by the additional constraint-release mechanism.

ACKNOWLEDGMENTS

The present work has been supported by the Deutsche Forschungsgemeinschaft (DFG) within the priority program SPP1369.

[1] M. Doi and S. F. Edwards, *The Theory of Polymer Dynamics* (Oxford University Press, USA, 1986).
[2] P. G. de Gennes, "Reptation of a polymer chain in the presence of fixed obstacles," J. Chem. Phys. **55**, 572–579 (1971).

[3]M. Doi, "Explanation for the 3.4-power law for viscosity of polymeric liquids on the basis of the tube model," J. Polym. Sci., Part B: Pol. Phys. **21**, 667–684 (1983).
[4]W. W. Graessley, "Entangled linear, branched and network polymer systems—Molecular theories," Adv. Polym. Sci. **47**, 67–117 (1982).
[5]C.-Y. Liu, R. Keunings, and C. Bailly, "Do deviations from reptation scaling of entangled polymer melts result from single- or many-chain effects?," Phys. Rev. Lett. **97**, 246001 (2006).
[6]S. T. Milner and T. C. B. McLeish, "Reptation and contour-length fluctuations in melts of linear polymers," Phys. Rev. Lett. **81**, 725–728 (1998).
[7]M. Doi, W. W. Graessley, E. Helfand, and D. S. Pearson, "Dynamics of polymers in polydisperse melts," Macromolecules **20**, 1900–1906 (1987).
[8]G. Marrucci, "Relaxation by reptation and tube enlargement: A model for polydisperse polymers," J. Polym. Sci., Part B: Pol. Phys. **23**, 159–177 (1985).
[9]J. L. Viovy, M. Rubinstein, and R. H. Colby, "Constraint release in polymer melts: Tube reorganization versus tube dilation," Macromolecules **24**, 3587–3596 (1991).
[10]R. C. Picu and A. Rakshit, "Coarse grained model of diffusion in entangled bidisperse polymer melts," J. Chem. Phys. **127**, 144909 (2007).
[11]Z. Wang and R. G. Larson, "Constraint release in entangled binary blends of linear polymers: A molecular dynamics study," Macromolecules **41**, 4945–4960 (2008).
[12]K. Kremer and G. S. Grest, "Dynamics of entangled linear polymer melts: A moleculardynamics simulation," J. Chem. Phys. **92**, 5057–5086 (1990).
[13]R. D. Groot and P. B. Warren, "Dissipative particle dynamics: Bridging the gap between atomistic and mesoscopic simulation," J. Chem. Phys. **107**, 4423–4435 (1997).
[14]N. A. Spenley, "Scaling laws for polymers in dissipative particle dynamics," Europhys. Lett. **49**, 534–540 (2000).
[15]G. Pan and C. W. Manke, "Developments toward simulation of entangled polymer melts by dissipative particle dynamics (DPD)," Int. J. Mod. Phys. B **17**, 231–235 (2003).
[16]J. T. Padding and W. J. Briels, "Uncrossability constraints in mesoscopic polymer melt simulations: Non-Rouse behavior of $C_{120}H_{242}$," J. Chem. Phys. **115**, 2846–2859 (2001).
[17]M. Langeloth, Y. Masubuchi, M. C. Böhm, and F. Müller-Plathe, "Recovering the reptation dynamics of polymer melts in dissipative particle dynamics simulations via slipsprings," J. Chem. Phys. **138**, 104907 (2013).
[18]Y. Masubuchi, J. Takimoto, K. Koyama, G. Ianniruberto, F. Greco, and G. Marrucci, "Brownian simulations of a network of reptating primitive chains," J. Chem. Phys. **115**, 4387–4394 (2001).
[19]Y. Masubuchi, H. Watanabe, G. Ianniruberto, F. Greco, and G. Marrucci, "Comparison among slip-link simulations of bidisperse linear polymer melts," Macromolecules **41**, 8275–8280 (2008).
[20]P. J. Hoogerbrugge and J. M. V. A. Koelman, "Simulating microscopic hydrodynamic phenomena with dissipative particle dynamics," Europhys. Lett. **19**, 155–160 (1992).
[21]D. Frenkel and B. Smit, *Understanding Molecular Simulation* (Academic, London, 2002).
[22]V. C. Chappa, D. C. Morse, A. Zippelius, and M. Müller, "Translationally invariant slip-spring model for entangled polymer dynamics," Phys. Rev. Lett. **109**, 148302 (2012).
[23]T. Uneyama and Y. Masubuchi, "Multi-chain slip-spring model for entangled polymer dynamics," J. Chem. Phys. **137**, 154902 (2012).
[24]A. Ramírez-Hernández, M. Müller, and J. J. de Pablo, "Theoretically informed entangled polymer simulations: linear and non-linear rheology of melts," Soft Matter **9**, 2030–2036 (2013).
[25]P. Español and P. Warren, "Statistical mechanics of dissipative particle dynamics," Europhys. Lett. **30**, 191–196 (1995).
[26]M. Pütz, K. Kremer, and G. S. Grest, "What is the entanglement length in a polymer melt?," Europhys. Lett. **49**, 735–741 (2000).
[27]S. Wang, E. D. von Meerwall, S.-Q. Wang, A. Halasa, W.-L. Hsu, J. P. Zhou, and R. P. Quirk, "Diffusion and rheology of binary polymer mixtures," Macromolecules **37**, 1641–1651 (2004).
[28]M. Rubinstein and R. H. Colby, *Polymer Physics* (Oxford University Press, USA, 2003).
[29]A. E. Likhtman, M. S. Talib, B. Vorselaars, and J. Ramirez, "Determination of tube theory parameters using a simple grid model as an example," Macromolecules **46**, 1187–1200 (2013).
[30]V. R. Raju, E. V. Menezes, G. Marin, W. W. Graessley, and L. J. Fetters, "Concentration and molecular weight dependence of viscoelastic properties in linear and star polymers," Macromolecules **14**, 1668–1676 (1981).
[31]D. Auhl, P. Chambon, T. C. B. McLeish, and D. J. Read, "Elongational flow of blends of long and short polymers: Effective stretch relaxation time," Phys. Rev. Lett. **103**, 136001 (2009).
[32]H. Watanabe, S. Ishida, Y. Matsumiya, and T. Inoue, "Test of full and partial tube dilation pictures in entangled blends of linear polyisoprenes," Macromolecules **37**, 6619–6631 (2004).
[33]R. H. Colby and M. Rubinstein, "Two-parameter scaling for polymers in Θ solvents," Macromolecules **23**, 2753–2757 (1990).
[34]E. van Ruymbeke, Y. Masubuchi, and H. Watanabe, "Effective value of the dynamic dilution exponent in bidisperse linear polymers: from 1 to 4/3," Macromolecules **45**, 2085–2098 (2012).
[35]R. J. A. Steenbakkers, C. Tzoumanekas, Y. Li, W. K. Liu, M. Kröger, and J. D. Schieber, "Primitive-path statistics of entangled polymers: mapping multi-chain simulations onto single-chain mean-field models," New J. Phys. **16**, 015027 (2014).
[36]S. T. Milner, "Predicting the tube diameter in melts and solutions," Macromolecules **38**, 4929–4939 (2005).
[37]H. Watanabe and T. Kotaka, "Viscoelastic properties and relaxation mechanisms of binary blends of narrow molecular weight distribution polystyrenes," Macromolecules **17**, 2316–2325 (1984).
[38]S. Wang, S.-Q. Wang, A. Halasa, and W.-L. Hsu, "Relaxation dynamics in mixtures of long and short chains: Tube dilation and impeded curvilinear diffusion," Macromolecules **36**, 5355–5371 (2003).

Dissipative particle dynamics simulation with slip-springs predicts the rheology of entangled polymers in solution

Michael Langeloth,*,†,‡ Yuichi Masubuchi,‡ Michael C. Böhm,† and Florian Müller-Plathe†

Eduard-Zintl-Institut für Anorganische und Physikalische Chemie and Center of Smart Interfaces, Technische Universität Darmstadt, Alarich-Weiss-Strasse 4, 64287 Darmstadt, Germany, and Institute for Chemical Research, Kyoto University, Gokasho, Uji 611-0011, Japan

E-mail: m.langeloth@theo.chemie.tu-darmstadt.de

*To whom correspondence should be addressed

†Eduard-Zintl-Institut für Anorganische und Physikalische Chemie and Center of Smart Interfaces, Technische Universität Darmstadt, Alarich-Weiss-Strasse 4, 64287 Darmstadt, Germany

‡Institute for Chemical Research, Kyoto University, Gokasho, Uji 611-0011, Japan

Abstract

We use a combination of dissipative particle dynamics (DPD) and slip-springs to describe solutions of polymers of different chain lengths and concentrations in an explicit solvent. The DPD method is used both for speed and for its ability to correctly handle hydrodynamics; slip-springs are used to mimic entanglements of polymer chains. Our earlier model developed for polymer melts is here augmented by a prescription which obtains the slip-spring density as a function of polymer concentration. With this modification, the model is able to describe the viscoelastic behaviour of polymer solutions from the near-dilute regime through to the melt. The simulated polymer dynamics follows the Zimm behaviour for low polymer concentrations and, hence, low slip-spring densities. This behaviour is caused by the hydrodynamic interactions transmitted by the solvent molecules. The entangled behaviour gradually appears with increasing slip-spring density. In the entangled state, the elastic behaviour sets in and the plateau modulus scales with the polymer concentration with an exponent of 2.0 to 2.3. We demonstrate the validity of the proposed slip-spring model in polymer solutions by the superposition of the storage and loss moduli. In this way, we show that the polymer dynamics is universal for chains that bear the same number of slip-springs. The universality is obtained because of the inclusion of the hydrodynamic interactions in DPD simulations. The behaviour also agrees qualitatively with experimental results. Owing to the slip-spring functionality and their fluctuations, however, their number density is close to, but not equivalent to the number density of entanglements derived from experiments by various models and assumptions.

Introduction

The polymer chains in a solution are far apart at a low polymer volume fraction φ. In this situation, their dynamics follows the prediction of the Zimm model[1] because they cannot entangle with each other.[2,3] The Zimm model[1] is an extension of the Rouse model[4] and includes hydrodynamic interactions. At higher φ, the distance between the chains becomes smaller until they penetrate each other. This causes the formation of entanglements which constrain the dynamics of the chains. In concentrated polymer solutions, the hydrodynamic interactions become negligible. Instead, the dynamics then rather corresponds to the behaviour in polymer melts, which is dominated by reptation dynamics.[2,3]

The established analytical models[1–4] are restricted to either entangled or dilute polymer systems. A unified picture that applies to both, Zimm and reptation dynamics, including the crossover region, is still missing. This gap can be closed by molecular dynamics simulations. Full atomistic molecular dynamics describes correctly polymer chains in solutions and melts. The large time and length scales, however, make it unfeasible to run such simulations long enough to observe all aspects of polymer dynamics. Coarse-grained or mesoscopic polymer models are often used to reduce the computational requirements. Coarse-grained Lennard-Jones bead-spring models, such as the Kremer-Grest polymer chains,[5] exhibit entangled dynamics. However, those simulations still require massive computational effort, even if the chain lengths are limited to only a few entanglement lengths.[6] Mesoscopic simulation models such as dissipative particle dynamics (DPD)[7,8] are much faster because they use an even more coarse-grained description of the chain: each bead does not represent an atom or a monomeric unit, but an entire chain segment. While mesoscopic approaches make simulations of longer chain lengths affordable, they do not consider entanglements. This is due to the inevitable softness of mesoscopic potentials, which are incapable of preventing chains from crossing each other. Therefore, the chains show no signs of entangled dynamics and move according to the Rouse or Zimm model,[1,4] irrespective of their length.[9] Attempts have been made to enforce the uncrossability of chains on mesoscopic models, by for example the segmental repulsive

potential[10] and the TWENTANGLEMENT[11] method. However, these approaches either limit the degree of coarse-graining of the polymer model or are computationally expensive.

Recently, slip-link and slip-spring methods have become popular. They offer an easy way to artificially add entanglement-like constraints to a polymer melt. In the present study we use our multi-chain slip-spring approach for DPD that has already shown to reproduce the correct dynamical behaviour of entangled and unentangled chains for mono- and bidisperse melts.[12,13] Similar multi-chain approaches that also implement slip-springs into DPD have been developed by Chappa et al.[14] and very recently by Nikoubashman et al.[15] Other multi-chain approaches which are based on Brownian dynamics[16] or field methods[17], cannot capture hydrodynamic interactions, as they do not locally conserve the momentum. An extensive summary of the current state of the art has been published by one of the present authors.[18]

In comparison to conventional polymer models that prevent chain crossings by excluded volume interactions,[5] our slip-spring approach has shown to be two orders of magnitude faster.[12] It also has advantage over tube models or conventional slip-link models, as these require the determination of a time (friction coefficient, relaxation time) and stress scale (entanglement mesh size, entanglement molecular weight or the plateau modulus).[19] This is extremely unfavourable for simulations of dilute polymers as both scales are affected by the concentration of solvent molecules. DPD simulations, however, do not require knowledge of these two parameters. In fact, we demonstrate that these two scales are obtained readily from the dynamics. In other words, they are output, rather than input parameters of the simulations. The multi-chain slip-spring model for DPD appears to be, therefore, presently the only one that can correctly screen various polymer concentrations from dilute solutions with hydrodynamic interactions to concentrated polymer solutions which behave like in a melt.

We demonstrate the validity of our model for polymer solutions by analysing the viscoelastic behaviour of systems with different volume fractions and molecular weights. The

universal behaviour of the storage and loss moduli ($G'(\omega)$ and $G''(\omega)$) for chains that bear the same number of entanglements is a characteristic attribute of polymer solutions. The viscoelastic response functions of different simulations agree almost perfectly. However, the results suggest that the number of entanglements derived from experiments is not necessarily equal to the number of slip-springs. It is assumed that this discrepancy between the number of entanglements and slip-springs is model dependent.[19,20]

Method

Dissipative particle dynamics has been developed by Hoogerbrugge and Koelman[7] and later improved by Groot and Warren[8]. It is a mesoscopic simulation method which distinguishes itself by a thermostat that conserves momentum locally. In this way, the DPD method can correctly describe hydrodynamic interactions and thus, is suitable for simulations of polymer solutions. The DPD method is same as in our previous publications[12,13] and has been thoroughly described by Groot and Warren[8]. Reduced units are used throughout this article, by which bead mass m, force cutoff distance r_c and k_BT are all equal to 1.

Owing to the DPD potential being soft, the nonbonded forces are too weak to avoid DPD chains from crossing each other. Consequently, this unphysical behaviour leads to an unentangled polymer dynamics regardless of the chain length as Spenley[9] demonstrated for melts. We have shown in previous publications that slip-springs can compensate the loss of the entanglement effect in polymer melts of monodisperse[12] and bidisperse[13] chains. The chains with a molecular weight above a critical molecular weight exhibit correct reptation dynamics when slip-springs are employed. The dynamics of chains below the critical weight remains qualitatively the same.

The slip-springs are modelled by a harmonic potential, identical to the spring potential between neighbouring chain beads. Initially, the slip-springs are distributed randomly over the simulation cell. They connect beads that are sufficiently close to each other; the two

beads may belong to different chains or the to same chain. In contrast to the permanent cross-links of a polymeric network, the position of the slip-springs is not fixed. The dynamics include a sliding motion of the slip-springs along the chains as well as the creation and destruction of slip-springs at the chain ends, i.e. changes of the system's Hamiltonian. The simulation protocol alternates between DPD sequences, where the beads are moving with a fixed slip-spring topology, and Monte-Carlo (MC)[21] sequences, where the position of the chain beads is frozen and only the slip-spring positions are allowed to change. Thus, the slip-spring dynamics is treated independently from the DPD chain beads dynamics.

The two mounting points of a slip-spring may jump from bead to bead in random direction along the chains. This migration is governed by a MC algorithm which uses the Metropolis criterion[21] as an acceptance rule. Different slip-springs do not interact with each other. Therefore, it might happen that two or more slip-springs are mounted on the same bead or that two slip-springs pass through each other. A slip-spring can be destroyed at the end of a MC sequence if at least one mounting point has reached a chain end. However, a new slip-spring must then be created at some other randomly selected chain end. Therefore the number of slip-springs remains constant throughout the simulation as there is no single process that destroys or creates slip-springs independently. This relocation process is governed by the Metropolis criterion, too. Detailed balance[21] is ensured at all times. A more thorough discussion about the slip-spring dynamics and its implementation is provided in one of our previous publications.[12] The approach used here is almost identical, with the only restriction that we do not allow slip-spring connections with solvent monomers. Hence, the solvent molecules are not supposed to contribute to the overall confinement of the chains.

The number of inserted slip-springs depends on the volume fraction φ of the chains. For the melt systems we choose the average molecular weight between two slip-springs to be five beads. The average number of slip-springs per chain is therefore $Z = 10, 15$ and 20 for chains with a molecular weight of $M = 50, 75$ and 100, respectively. In the presence of solvent beads the number of slip-springs must be reduced. Firstly, because the number density of chain

beads decreases with reduced polymer volume fraction and hence, the number of possible interaction sites decreases as well, as we do not allow a slip-spring connection to a solvent bead. Secondly, it has been derived from experiments[22] that the molecular weight between two entanglements inside a chain increases with reduced volume fraction. Taking both effects into account, the total number of slip-springs in the system n_{ss} should increase with increasing volume fraction as:

$$n_{ss}(\varphi) = n_{ss}(1)\varphi^{1+\alpha}. \tag{1}$$

The precise value of the dilution exponent α is still a matter of debate, but it is assumed to be somewhere in the range of $1.0 \leq \alpha \leq 1.3$.[23–25] We choose the dilution exponent to be at the upper limit with $\alpha = 1.3$. With this choice, we follow the Colby-Rubinstein conjecture for θ solvents.[26,27] We investigate chains in polymer solutions with various molecular weight and volume fractions. The molecular weight is varied over three different lengths with $M = 50, 75$ and 100 beads. The volume fraction of the chains is in the range of $0.3 \leq \varphi \leq 1$. Table 1 shows the average number of slip-springs per chain Z for all systems considered. All systems were equilibrated for 20 million DPD time steps without slip-springs to benefit from the faster dynamics. After that, a production run of 100 million DPD steps has been carried out with intervening slip-spring relocation.

Simulation details

The simulation cell consists of solvent and chain beads. The masses and the nonbonded interactions are identical for both bead types. Thus, the solvent can be regarded as a θ solvent. Although, it would be possible to study other solvent qualities, too. The repulsion parameter is $a_{ij} = 25k_BT$. Chain beads are coupled with a spring constant of $k = 2k_BT/(r_c)^2$. The same spring constant is also used for the slip-spring interaction. The integration is performed with a time step of $\Delta t = 0.06\tau$, with τ being the time unit $\tau = (r_c^2 m/k_BT)^{0.5}$. The noise

Table 1: Average number of slip-springs per chain Z

φ^b/%	Z		
	M^a=50	M^a=75	M^a=100
30	2.1	3.1	4.2$^\bullet$
50	4.1$^\bullet$	6.1	8.2$^\diamond$
70	6.3	9.5*	12.6
85	8.1$^\diamond$	12.1	16.1
90	8.7	13.0	17.4
95	9.4*	14.0	18.7
100	10.0	15.0	20.0

[a] Molecular weight of the polymer chains. The mass of an individual bead equals unity.
[b] Volume fraction of the polymer chains.
$^{\star,\diamond,\bullet}$ Sets with similar Z.

amplitude for the DPD thermostat is set to $\sigma = 3k_BT(\tau)^{0.5}$. The size of the simulation cell is $48r_c \times 12r_c \times 12r_c$ with periodic boundary conditions in all dimensions. We confirm that the cuboid shape does not affect the results presented below.The number of DPD beads is 20700 for a pure melt with $\varphi = 1$ and 20736 for any other polymer solution with $\varphi < 1$. The density is close to $\rho = 3r_c^{-3}$.

Results and discussion

Plateau modulus

Figure 1 shows the relaxation modulus $G(t)$ for a few selected volume fractions of the chains with a molecular weight of $M = 50$. The behaviour of the two other chain lengths is qualitatively the same and thus not shown here. The relaxation modulus has been calculated from the stress tensor, which consists of contributions from all pair interactions including the slip-springs. $G(t)$ is the autocorrelation function of the non-diagonal elements of the stress tensor, $\boldsymbol{\sigma}_{\alpha,\beta}$ with V being the volume of the system (2). In spite of the use of cuboid cell, the correlation functions obtained from different shear components are essentially the same so that $G(t)$ presented below is the average of the correlation functions.

$$G(t) = \frac{V}{k_B T} \langle \boldsymbol{\sigma}_{\alpha,\beta}(t) \boldsymbol{\sigma}_{\alpha,\beta}(0) \rangle, \; \alpha \neq \beta \tag{2}$$

Each volume fraction is depicted with different symbols in Figure 1. It has been experimentally observed that the plateau modulus G_N^0 is reduced in the presence of a solvent as shown in equation (3).[22,28] The dilution exponent α usually takes values between 1.0 and 1.3 depending on the model used to analyse the experimental data.[23–25]

$$G_N^0 \propto \varphi^{(1+\alpha)} \tag{3}$$

The reason for the concentration dependence of G_N^0 is, next to the chain density, also the formation of more entanglements at higher polymer concentration. Solvent molecules in the vicinity of a chain, on the other hand, do not impose any constraints and therefore lead to fewer entanglements. The plateau values G_N^0 have been extracted from $G(t)$ together with the relaxation time τ_d on the basis of the pure reptation spectrum[3] as proposed by del Biondo et al.[29] The values for the systems with $M = 50$ have been marked by black stars to the relaxation modulus in Figure 1. Figure 2 shows the values of the plateau modulus and the relaxation time for all three chain lengths at various volume fractions φ. The straight lines are guides to the eye and illustrate the scaling behaviour. The plateau modulus is fairly independent of the molecular weight given that the polymer concentration is sufficient to attain the entangled dynamics. It scales against φ with an exponent close to the experimental relation in equation (3)[28] with α being in the range of 1.0 and 1.3. The relaxation time τ_d on the right side of Figure 2 scales with an exponent of approximately 1.3. However, the scaling exponents may take other values if a different method is applied for the extraction of G_N^0 and τ_d.

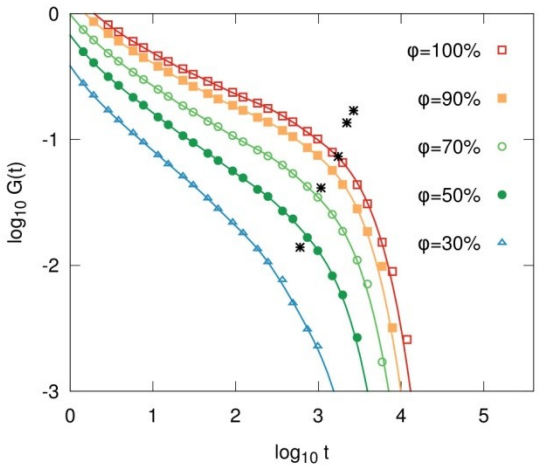

Figure 1: Relaxation modulus $G(t)$ for polymer solutions with $M = 50$ and various volume fractions φ. The points are the actual simulation results. The full curves are fits to a multi-exponential decay function. The black stars show from top to bottom the results of G_N^0 against τ_d for $\phi = 100\%$ to 30%.

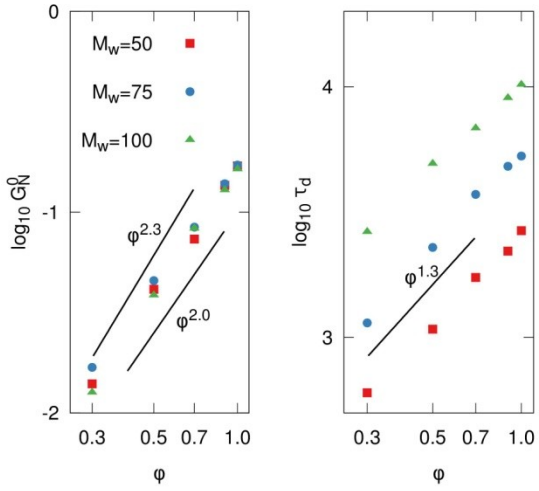

Figure 2: Plateau modulus G_N^0 and relaxation time τ_d for various chain lengths in solution. The straight lines are guides to the eye to illustrate different scaling behaviours.

Storage and loss moduli

We further analyse the viscoelastic behaviour by calculating the storage and loss moduli, $G'(\omega)$ and $G''(\omega)$. The conversion of $G(t)$ into $G'(\omega)$ and $G''(\omega)$ has been done by first fitting $G(t)$ to an exponential decay function with 6 modes and then Fourier-transforming

this function. The results of this fit are shown in Figure 1 as full curves and match the simulation results quite well. The loss and storage moduli of all available volume fractions with chain length $M = 50$ are shown in Figure 3 against the frequency ω. The curves have been shifted vertically to avoid overlapping. The straight horizontal lines mark the height where $\log_{10} G'(\omega)$ or $\log_{10} G''(\omega)$ equal -1.

The storage and loss moduli in the high frequency region continue parallel for volume fractions below 50%. The straight black line is a guide to the eye and has an exponent of 2/3. This scaling corresponds to the Zimm behaviour in θ solutions[22] and agrees very nicely with $G'(\omega)$ and $G''(\omega)$ at higher frequencies. At concentrations above 50%, both moduli cross each other in the low frequency regime. This effect is accompanied by the development of a plateau in $G(t)$, see Figure 1. The crossover appears when the polymer chains start to entangle and it marks the onset of the elastic behaviour at higher frequencies. The width of this elastic region, which is enclosed by the two crossover points in the low and high frequency regime, increases with φ as the chains become more and more entangled. The behaviour for the other two chain lengths with $M = 75$ and 100 differs only in the way that the entanglement coupling begins at a lower concentration and that the distance between both crossover points is wider.

Superposition

The shapes of the modulus curves depend on the molecular weight and the volume fraction. The influence of both, however, can be effectively summarized by the average number of entanglements per chain. This universality means that the hydrodynamic interaction does not appear in the viscoelastic function. Conventional slip-link or slip-spring models neglect the hydrodynamic interactions, and thus, the universality must be assumed a priori. However, in our model, we explicitly calculate the hydrodynamic interactions so that the universality is not guaranteed. In this section, we test the universality by the superposition of different viscoelastic spectra with various M_e or φ but identical number of slip-springs per chain Z

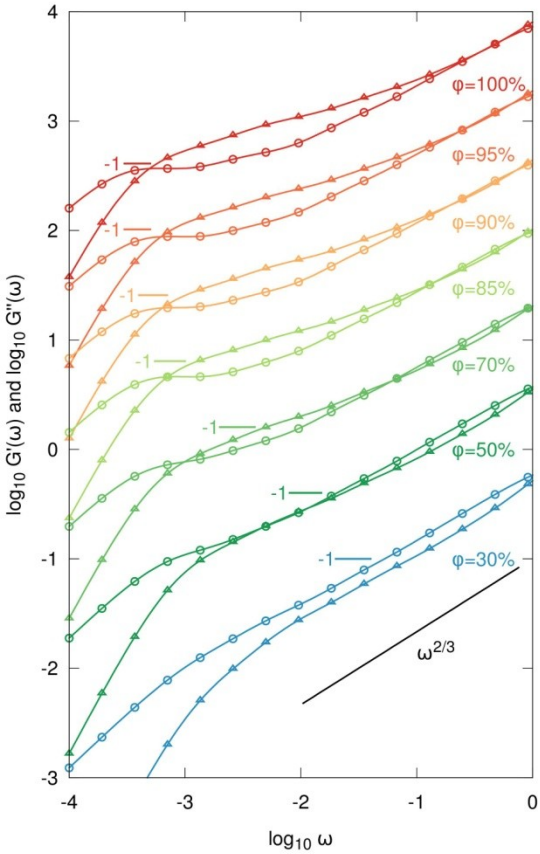

Figure 3: Storage (triangles) and loss (circles) modulus, $G'(\omega)$ and $G''(\omega)$, of polymer solutions with $M = 50$ and various volume fractions ranging from $\varphi = 100\%$ to 30% from top to bottom. The curves have been shifted vertically to avoid overlapping. The straight black line shows the Zimm behaviour with a scaling of 2/3.

as shown by Heo and Larson[30] as well as Huang et al.[28] They both normalized $G'(\omega)$ and $G''(\omega)$ by the plateau modulus G_N^0 and the frequency ω by the inverse entanglement time $1/\tau_e$. Here, for convenience we scale both axes with the φ dependence of G_N^0 and τ_e, instead. The scaling of the plateau modulus with volume fraction is illustrated in equation (3). The entanglement time scales with φ as $\tau_e \propto \varphi^{1-2\alpha}$.[30] For the scaling of both axes we use a value of 1.3 for the dilution exponent α. Table 1 lists all Z values for the systems described here, with Z being the average number of slip-springs on a chain. In this table, there are some systems that have very similar Z values. Those systems are marked with different symbols,

i.e. star, diamond or circle and are shown in Figure 4. The three sets have been shifted vertically for the sake of clearness. The superposition matches surprisingly good for all three combinations of Z with only slight deviations. At this point, we would like to emphasize that Figure 4 shows that the proper scaling of the time and stress constants is obtained without the need of additional parameters. Unlike other tube or conventional slip-link models, the solvation of the polymer chains is taken into account a posteriori in DPD simulations.

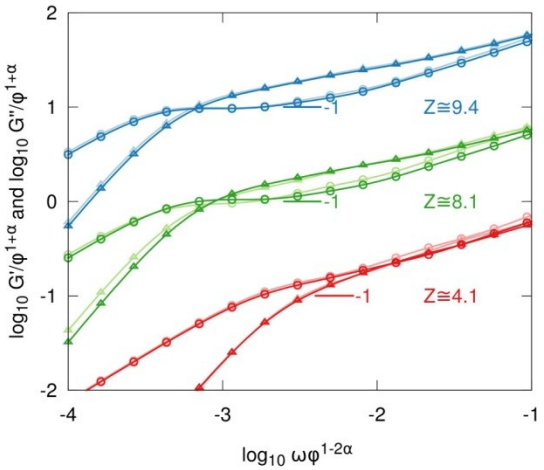

Figure 4: Superposition of $G'(\omega)$ and $G''(\omega)$. The blue, green and red curves each show the results of the two systems in Table 1 marked with stars, diamonds or circles. The curves have been shifted vertically to avoid overlapping.

Superposition with experiments

The universal behaviour of polymer solutions also facilitates a comparison of the slip-spring simulations with experimental results. Figure 5 shows the viscoelastic response functions of polystyrene chains in solution with $Z = 9.4$ (blue curves) from Huang et al.[28] The regime between the two crossover points is too wide, compared to simulations where the number of slip-springs is identical to the inferred number of entanglements per chain in experimental polystyrene. If, however, the number of slip-springs is twice the number of (experimental) entanglements, the curves match very well. This situation is illustrated in Figure 5 for a

solution with $\varphi = 95\%$ and chains with a mass of $M = 100$ (red curves). Since $G'(\omega)$ and $G''(\omega)$ of various simulations with different φ have been successfully superimposed (see Figure 4), we feel confident that the superposition with experimental data could be achieved for lower volume fractions as well. A very similar relation between the number of slip-links and experimental entanglements has been observed by Masubuchi et al.[19] for the multi-chain slip-link model. Although, their slip-link implementation of an entanglement differs from our slip-spring model, similar relations of the artificial entanglements seem reasonable considering the mechanical force balance around the entanglement in both models. As pointed out by Schieber el al.,[20] the determination of Z from the plateau modulus is not straightforward. The relationships between G_N^0 and M_e are model dependent and differ by a coefficient ν as shown in equation (4), with ρ being the chain density and R being the gas constant.[19]

$$G_N^0 = \nu \frac{\rho RT}{M_e} \tag{4}$$

From equations (3) and (4) it follows that the entanglement weight M_e also depends on the volume fraction φ as:

$$M_e(\varphi) = M_e(1)\varphi^{-\alpha}. \tag{5}$$

The coefficient depends on the functionality of the entanglements in terms of their connectivity as well as the entanglement fluctuations.[19] The functionality of entanglements and their fluctuations are mainly unknown as there is still no consensus of what an entanglement really is. The theory of rubber elasticity considers entanglements as cross-links like in a polymeric network. The model uses a coefficient of $\nu = 1.0$ and does not consider any entanglement fluctuations because of the quasi-permanent topology of the cross-links. The tube model of Doi and Edwards considers only a few fluctuations such as contour-length fluctuations and uses a coefficient of $\nu = \frac{4}{5}$.[3] However, the influence of single fluctuations on the coefficient is hard to determine.[20] Huang et al. determined the dilution exponent

from linear viscoelastic data and found best agreement for $\alpha = 1.0$.[28] Hence, Z reported by Huang et al. has been calculated from the value of the pure melt by using equation (5) with $\alpha = 1.0$.[28] The melt value has been derived from G_N^0 by using the relation from rubber elasticity (equation (4) with $\nu = 1.0$)[31]. The reason for the different dilation exponents in our slip-spring model and the experimental data of Huang et al. might be attributed to the solvent mobility. However, this question cannot be answered conclusively at this point in time. The discussion shows that the determination of Z from experimental data depends on the theoretical model applied. Likewise, we assume that the relationship between G_N^0 and M_e in the present slip-spring simulation depends on the implementation of the slip-springs. It is therefore not required or even anticipated that chains which produce the same viscoelastic responce have the identical number of entanglements and slip-springs.

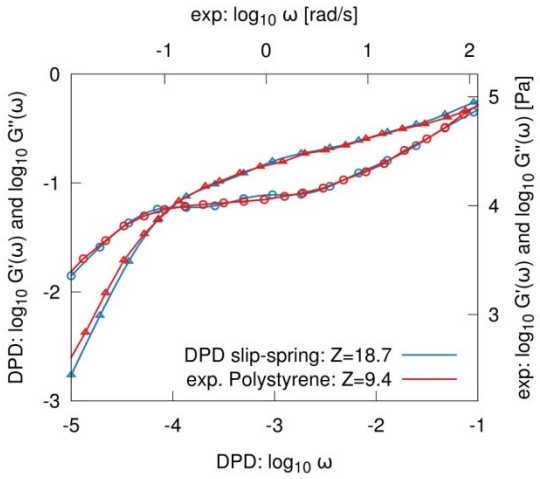

Figure 5: Superposition of $G'(\omega)$ and $G''(\omega)$. The red curves are the results of a DPD solution with $M = 100$ and $\varphi = 95\%$. The blue curves are the experimental data from Huang et al.[28] of a polystyrene solution with $Z = 9.4$.

Conclusion

The present manuscript demonstrates the applicability of our slip-spring model to polymer solutions of varying polymer concentration. Other existing slip-spring or slip-link models

often cannot capture the hydrodynamic interactions because their simulation method does not conserve the momentum. The implementation into DPD[7,8], however, offers an easy and fast way to describe solvation effects without the need of additional parameters. We show the relaxation modulus and the storage and loss moduli of polymer solutions at various volume fractions. The concentration range covers almost unentangled solutions that exhibit Zimm dynamics as well as concentrated solutions with a pronounced entanglement coupling.[22] In the entangled regime, the plateau modulus scales with the volume fraction φ with an exponent ranging between 1.0 and 1.3 for all three chain lengths investigated. The formation and widening of the elastic region between both crossover points in $G'(\omega)$ and $G''(\omega)$ is clearly visible at high concentrations. This behaviour marks the onset of the entanglement coupling as the chains begin to penetrate each other. In addition, we observe the universality of the viscoelastic response functions[28,30] at different polymer concentrations, for chains that bear the same number of slip-springs. We want to emphasize that we obtain the universality, because the hydrodynamic interactions are explicitly considered in DPD simulations. The viscoelastic responce functions also superpose well with experimental results, but the number of slip-springs may not be equivalent to the number of experimentally derived entanglements. This is mainly due because the entanglement description in the model which has been applied to the experimental data is not consistent with the implementation of the slip-springs and their dynamics.[19,20] Nevertheless, additional tests against experiments are apparently necessary for various solvent quality and mobility. Moreover, the effect of parameters like the spring constant or the slip-spring mobility should be examined, too. We are continuing our study in these directions and the results will be published elsewhere.

Acknowledgement

The authors highly appreciate the financial support from the Institute for Chemical Research at Kyoto University and from the Deutsche Forschungsgemeinschaft (DFG) within the priority program SPP1369.

References

(1) Zimm, B. *The Journal of Chemical Physics* **1956**, *24*, 269–278.

(2) de Gennes, P. G. *The Journal of Chemical Physics* **1971**, *55*, 572–579.

(3) Doi, M.; Edwards, S. F. *The Theory of Polymer Dynamics*; Oxford University Press, USA, 1986.

(4) Rouse, P. E. *The Journal of Chemical Physics* **1953**, *21*, 1272–1280.

(5) Kremer, K.; Grest, G. S. *The Journal of Chemical Physics* **1990**, *92*, 5057–5086.

(6) Likhtman, A. E.; Sukumaran, S. K.; Ramirez, J. *Macromolecules* **2007**, *40*, 6748–6757.

(7) Hoogerbrugge, P. J.; Koelman, J. M. V. A. *Europhysics Letters* **1992**, *19*, 155–160.

(8) Groot, R. D.; Warren, P. B. *The Journal of Chemical Physics* **1997**, *107*, 4423–4435.

(9) Spenley, N. A. *Europhysics Letters* **2000**, *49*, 534–540.

(10) Pan, G.; Manke, C. W. *International Journal of Modern Physics B* **2003**, *17*, 231–235.

(11) Padding, J. T.; Briels, W. J. *Journal of Chemical Physics* **2001**, *115*, 2846–2859.

(12) Langeloth, M.; Masubuchi, Y.; Böhm, M. C.; Müller-Plathe, F. *The Journal of Chemical Physics* **2013**, *138*, 104907.

(13) Langeloth, M.; Masubuchi, Y.; Böhm, M. C.; Müller-Plathe, F. *The Journal of Chemical Physics* **2014**, *141*, 194904.

(14) Chappa, V. C.; Morse, D. C.; Zippelius, A.; Müller, M. *Physical Review Letters* **2012**, *109*, 148302.

(15) Nikoubashman, A.; Davis, R. L.; Michal, B. T.; Chaikin, P. M.; Register, R. A.; Panagiotopoulos, A. Z. *ACS nano* **2014**, *8*, 8015–8026.

(16) Uneyama, T.; Masubuchi, Y. *Journal of Chemical Physics* **2012**, *137*, 154902.

(17) Ramírez Hernández, A.; Müller, M.; de Pablo, J. J. *Soft Matter* **2013**, *9*, 2030–2036.

(18) Masubuchi, Y. *Annual review of chemical and biomolecular engineering* **2014**, *5*, 11–33.

(19) Masubuchi, Y.; Ianniruberto, G.; Greco, F.; Marrucci, G. *Journal of Chemical Physics* **2003**, *119*, 6925–6930.

(20) Schieber, J. D.; Indei, T.; Steenbakkers, R. J. A. *Polymers* **2013**, *5*, 643–678.

(21) Frenkel, D.; Smit, B. *Understanding Molecular Simulation: From Algorithms to Applications*; Academic Press: London, 2002.

(22) Graessley, W. W. *Polymeric Liquids and Networks: Dynamics and Rheology*; Polymeric Liquids and Networks; Garland Science, 2008.

(23) Watanabe, H.; Ishida, S.; Matsumiya, Y.; Inoue, T. *Macromolecules* **2004**, *37*, 1937–1951.

(24) Van Ruymbeke, E.; Masubuchi, Y.; Watanabe, H. *Macromolecules* **2012**, *45*, 2085–2098.

(25) Van Ruymbeke, E.; Shchetnikava, V.; Matsumiya, Y.; Watanabe, H. *Macromolecules* **2014**, *47*, 7653–7665.

(26) Colby, R. H.; Rubinstein, M. *Macromolecules* **1990**, *23*, 2753–2757.

(27) Colby, R. H.; Rubinstein, M.; Viovy, J. L. *Macromolecules* **1992**, *25*, 996–998.

(28) Huang, Q.; Mednova, O.; Rasmussen, H. K.; Alvarez, N. J.; Skov, A. L.; Almdal, K.; Hassager, O. *Macromolecules* **2013**, *46*, 5026–5035.

(29) Del Biondo, D.; Masnada, E. M.; Merabia, S.; Couty, M.; Barrat, J. L. *Journal of Chemical Physics* **2013**, *138*, 194902.

(30) Heo, Y.; Larson, R. G. *Macromolecules* **2008**, *41*, 8903–8915.

(31) Bach, A.; Almdal, K.; Rasmussen, H. K.; Hassager, O. *Macromolecules* **2003**, *36*, 5174–5179.

Graphical TOC Entry

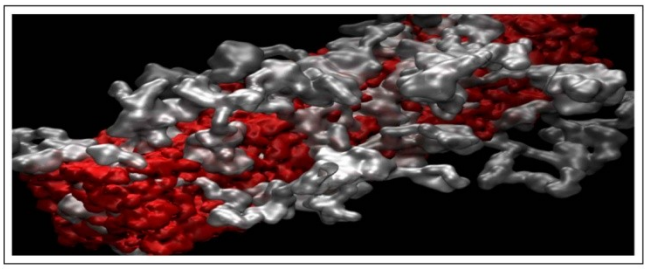

5. Conclusion:

We have proposed a new method to analyze entangled polymer dynamics in mesoscopic simulations. They usually fail to prevent unphysical chain crossings because the repulsion between two beads is too weak. This is a result of a high level of coarse-graining.[1,2] Thus, mesoscopic polymer chains show no signs of entanglement coupling, regardless of the chain length. The proposed method[3–5] does not retain the chain uncrossability. Instead, the loss of the entangled chain dynamics is compensated by the insertion of artificial bonds, so called slip-springs. These slip-springs connect two beads of nearby chains similar to the cross-links in a polymeric network. However, their position is not fixed. A slip-spring can jump along the chain in discrete steps from bead to bead. Additionally, slip-springs may also be created or destroyed at the chain ends. Within the last three chapters we have exposed our model to a variety of polymeric systems in order to validate its applicability in different environments.[3–5]

The first systems considered contain monodisperse, linear chains of various lengths. The chain statistics is not severely affected by the insertion of the slip-springs. The long chains have several slip-springs and move according to the tube theory. The mean-squared displacement of the central chain bead reveals the famous reptative regime with a scaling exponent of ¼.[6] The scaling behavior of the diffusion coefficient and the relaxation time agrees with the experimental relation of entangled chains, though the analysis does not allow to judge about the position after the decimal point.[7] The relaxation modulus indicates the formation of a plateau for the long chain lengths. The modulus can be superimposed with data from Kremer-Grest[8] simulations, where entanglements are considered through the excluded volume effects of the hard sphere beads. This benchmark test indicates that the proposed model is roughly 500 times faster compared to conventional methods such as Kremer-Grest. The dynamics of the short chains with a negligible number of slip-springs remains Rouse-like.

The second example of bidisperse, linear chains is a step towards the simulation of polydisperse systems and offers insight into additional relaxation processes that are less apparent in monodisperse simulations. The presence of the short chain component affects the relaxation of the long chains and vice versa. The slip-spring model confirms observations from a simulation with Kremer-Grest chains by Wang and Larson[9]. Moreover, the high efficiency of the present method facilitates large scale simulations with more disparate chain lengths and lower concentrations. This way, the slip-spring model successfully eradicates some discrepancies with theoretical models that resulted from the limited length scales in

Kremer-Grest[9] simulations. The composition of short and long chains is characterized by the Struglinsky-Graessley Parameter *Gr*. For systems with $Gr<1$, the constraint release effects become prominent soon after the relaxation of the short chains. However, the relaxation times of the long chains are not affected. Contrary to this, the relaxation times of the long chains scale linearly with the concentration for systems with more disparate chain lengths, i.e. $Gr<1$. The dynamics is on the whole reasonable and shows consistency with the theoretical predictions of tube dilation theory.[10,11]

The next chapter was about entanglement coupling in polymer solutions. The concentration ranged from low volume fractions with almost unentangled chains to concentrated polymer solutions. The former exhibited Zimm[12] behavior while the later showed considerable entanglement effects. The slip-spring density depends on the polymer concentration to account for this solvation effect. The plateau modulus and the relaxation times of various chain lengths and polymer concentrations are consistent with each other. The viscoelastic response of two simulations can be superimposed if the number of slip-springs per chain is similar for both.[13,14] We also show the superposition with experimental data and establish a relation between the number of slip-springs and entanglements. We want to emphasize that the proposed slip-spring model distinguishes itself from other slip-link or slip-spring models by that fact that the correct dynamic scaling of the time and stress constants with polymer concentration is obtained a posteriori without the need of additional parameters.

The validated systems facilitate numerous applications. The behavior is altogether reasonable and has been compared with Kremer-Grest[8] simulations, theoretical predictions or experimental observations. Although the proposed technique is about 500 times faster than conventional Kremer-Grest simulations, the computational gain appears less impressive if one considers that the relaxation time of a polymer chain in a melt scales with its molecular weight by an exponent of 3.4.[6] Thus, the relaxation time increases by a factor of ten if one doubles the chain length. The entanglement length in Kremer-Grest polymer chains lies somewhere in the range of 30 to 80 monomers, depending on the method that was used to extract the entanglement spacing from the simulation data.[15,16] Therefore, the number of entanglements in Kremer-Grest chains is typically limited to about 10 entanglements. Longer chain lengths require longer time scales and those are not feasible in MD simulations. In contrast to this, the chains in the proposed slip-spring model are limited to a maximum number of about 50 slip-springs. However, those numbers are just estimates to give a rough impression on the performance. More thorough examination is required for a more meaningful comparison. Still, even for moderately entangled chains the model allows several potential applications. For example, Nikoubashman *et al.* applied this approach to study

homo- and copolymers under shear.[17] It might also be worth to examine the validity of additional systems. It would be of great interest to see if the model is applicable to other architectures than linear chains, like for example branched or star polymers.[18] Presumably, the model can be applied to branched polymers with only small modifications. Based on the concept of arm retraction that has been established by de Gennes, we assume that the mounting points of a slip-spring must not pass the branching point of the polymer.[7] The behavior could be validated by measuring the viscosity of star polymers with varying number of arms and different arm lengths. The viscosity depends only on the number of entanglements per arm. It scales with an exponent of 3/2.[7] The number of arms, however, does not affect the relaxation time. Whether or not the proposed slip-spring model can be applied to ring polymers is also an interesting question.[19,20] However, it is expected that more severe modifications of the slip-spring algorithm, in particular for the slip-spring creation and destruction, are necessary to reproduce the experimental dynamics of ring polymers.

It would also be interesting to see how the polymer system behaves under shear flow. Shear flow can be applied in one direction by using for example Lees-Edwards boundary conditions[21] or reverse non-equilibrium MD[22]. Chappa *et al.*[23] measured the viscosity under shear flow for their DPD slip-spring model and found good agreement with experiments, including shear thinning. Their DPD model controls the number of slip-springs by a chemical potential. Hence, their simulation is carried out in an ensemble of varying slip-springs. They report that the number of slip-springs decreases slightly with the shear rate. This effect is anticipated from the tube model where it is assumed that the entanglements are pushed towards their chain ends under flow.[23] The number of slip-springs is constant in our simulations. In order to account for the disentanglement under shear flow, one possibility would be to adopt the chemical potential from Chappa *et al.*[23] Another alternative would be to establish a relationship between the number of slip-springs and the shear rate, similar to the approach we used for polymer solutions.[5] Simulations of polymer materials under flow are of particular interest for the polymer-processing industry which has a natural interest in reducing the energy cost for throughput.[1] Perhaps less obvious, but still of high commercial interest are such simulations for the food industry.[24,25]

The slip-spring approach might also be implemented into other simulation techniques. The particle field simulation of Milano and Kawakatsu[26] as well as Zhao *et al.*[27] is one promising example. Interactions between chains are considered through a potential mean field. Thus, the chains can pass through each other, like in the proposed DPD simulations. The technique facilitates simulations of chains with thousands of repeating units. The implementation of slip-springs in the particle field approach could offer insights into the rheology of entangled

chains on an atomistic level. However, slip-spring connections between the beads of different chains would require massive changes in the parallelization scheme.[27] In the current version of the code, the polymer chains are randomly assigned to a processor. As a result, a processor does not necessarily have the positions of other chain beads in the vicinity. For the calculation of the nonbonded interactions this was not necessary because the chain is interacting only with the particle field. However, the computation of the slip-spring interaction requires information about the bead position of different chains, which cannot be computed by a single processor without communication. In a first attempt, it would be most convenient to anchor a slip-spring to a fixed position in space as in the single chain slip-spring model of Likhtman.[28]

The combination of slip-springs and reactive MD[29], which served as the inspiration for the slip-spring model, allows for the simulation of linear polymerization reaction.[30] In contrast to previous MD studies[30] in our group, the slip-spring approach would facilitate much longer time and length scales. One fundamental problem of reactive MD is that the reaction must occur within the accessible time-scales of MD simulations, i.e. within a few nanoseconds. The slip-spring model might grant the chains more time for their relaxation between two successive reactions. Moreover, the polymerization reaction has been done only for short, unentangled chains so far. However, the transition from unentangled to entangled chain dynamics upon linear chain growth has an impact on the chain length distribution. Furthermore, The Trommsdorff-Norrish Effect is one example of an auto-acceleration in a radical polymerization reaction.[31,32] It is caused by a decrease of the termination rate for longer chain lengths and can lead to a dangerous rise in temperature. Especially the influence of branched polymer systems on the polymerization rate would be an interesting subject.[32]

Another promising opportunity for the slip-spring model would be to study interfaces in contact with entangled polymers. It is a very active field of today's research with various applications.[33–35] In particular nanoparticle composites are dominating the number of recently published articles in this field.[36–39] The effect of the nanoparticles on the entanglement density is still a matter of debate and probably depends on the polymer-nanoparticle interaction.[40,41] This issue might be difficult to approach through the current slip-spring approach because the entanglement spacing is predetermined as an input parameter. However, other phenomena like the diffusion of nanoparticles through the entanglement mesh of a polymer melt[41,42] or bridging effects of chains between two nearby particles on the viscosity[43] might be ideal applications for the slip-spring approach. We are confident that the significance of computer simulations in polymer science can benefit greatly through larger time and length scales.

References:

[1] Y. Masubuchi, Annu. Rev. Chem. Biomol. Eng. **5**, 11 (2014).

[2] J.T. Padding and W.J. Briels, J. Phys. Condens. Matter **23**, 233101 (2011).

[3] M. Langeloth, Y. Masubuchi, M.C. Böhm, and F. Müller-Plathe, J. Chem. Phys. **138**, 104907 (2013).

[4] M. Langeloth, Y. Masubuchi, M.C. Böhm, and F. Müller-Plathe, J. Chem. Phys. **141**, 194904 (2014).

[5] M. Langeloth, Y. Masubuchi, M.C. Böhm, and F. Müller-Plathe, Macromolecules **submitted**, (2015).

[6] M. Doi and S.F. Edwards, *The Theory of Polymer Dynamics* (Oxford University Press, USA, 1986).

[7] M. Rubinstein and R.H. Colby, Oxford Univ. Press. New York (2003).

[8] K. Kremer and G.S. Grest, J. Chem. Phys. **92**, 5057 (1990).

[9] Z. Wang and R.G. Larson, Macromolecules **41**, 4945 (2008).

[10] J.L. Viovy, M. Rubinstein, and R.H. Colby, Macromolecules **24**, 3587 (1991).

[11] M. Doi, W.W. Graessley, E. Helfand, and D.S. Pearson, Macromolecules **20**, 1900 (1987).

[12] B. Zimm, J. Chem. Phys. **24**, 269 (1956).

[13] Q. Huang, O. Mednova, H.K. Rasmussen, N.J. Alvarez, A.L. Skov, K. Almdal, and O. Hassager, Macromolecules **46**, 5026 (2013).

[14] Y. Heo and R.G. Larson, Macromolecules **41**, 8903 (2008).

[15] M. Pütz, K. Kremer, and G.S. Grest, Eur. Lett. **49**, 735 (1999).

[16] R.S. Hoy, K. Foteinopoulou, and M. Kröger, Phys. Rev. E **80**, 14 (2009).

[17] A. Nikoubashman, R.L. Davis, B.T. Michal, P.M. Chaikin, R.A. Register, and A.Z. Panagiotopoulos, ACS Nano **8**, 8015 (2014).

[18] E. van Ruymbeke, H. Lee, T. Chang, a Nikopoulou, N. Hadjichristidis, F. Snijkers, and D. Vlassopoulos, Soft Matter **10**, 4762 (2014).

[19] S. Gooßen, A.R. Brás, M. Krutyeva, M. Sharp, P. Falus, A. Feoktystov, U. Gasser, A. Wischnewski, and D. Richter, Phys. Rev. Lett. **113**, 168302 (2014).

[20] M. Kapnistos, M. Lang, D. Vlassopoulos, W. Pyckhout-Hintzen, D. Richter, D. Cho, T. Chang, and M. Rubinstein, Nat. Mater. **7**, 997 (2008).

[21] S.R. Rastogi and N.J. Wagner, Parallel Comput. **22**, 895 (1996).

[22] F. Müller-Plathe, Phys. Rev. E **59**, 4894 (1999).

[23] V.C. Chappa, D.C. Morse, A. Zippelius, and M. Müller, Phys. Rev. Lett. **109**, 148302 (2012).

[24] Z. V. Baines and E.R. Morris, Food Hydrocoll. **1**, 197 (1987).

[25] D.A. Pink and M.S.G. Razul, Food Struct. **1**, 71 (2014).

[26] G. Milano and T. Kawakatsu, J. Chem. Phys. **130**, 214106 (2009).

[27] Y. Zhao, A. De Nicola, T. Kawakatsu, and G. Milano, J. Comput. Chem. **33**, 868 (2012).

[28] A.E. Likhtman, Macromolecules **38**, 6128 (2005).

[29] K. Farah, F. Müller-Plathe, and M.C. Böhm, ChemPhysChem **13**, 1127 (2012).

[30] K. Farah, H.A. Karimi-Varzaneh, F. Müller-Plathe, and M.C. Böhm, J. Phys. Chem. B **114**, 13656 (2010).

[31] W.Y. Chiu, G.M. Carratt, and D.S. Soong, Macromolecules **16**, 348 (1983).

[32] G.D. Verros and D.S. Achilias, J. Appl. Polym. Sci. **111**, 2171 (2009).

[33] A. Karatrantos, R.J. Composto, K.I. Winey, M. Kröger, and N. Clarke, Macromolecules **45**, 7274 (2012).

[34] T. Ge, M.O. Robbins, D. Perahia, and G.S. Grest, Phys. Rev. E **90**, 1 (2014).

[35] S.M. Sabzevari, I. Cohen, and P.M. Wood-Adams, Macromolecules **47**, 8033 (2014).

[36] E. Masnada, S. Merabia, M. Couty, and J.-L. Barrat, Soft Matter **9**, 10532 (2013).

[37] G.D. Hattemer and G. Arya, Macromolecules **48**, 1240 (2015).

[38] S. Alam and A. Mukhopadhyay, Macromolecules **47**, 6919 (2014).

[39] J. Choi, M.J. a Hore, J.S. Meth, N. Clarke, K.I. Winey, and R.J. Composto, ACS Macro Lett. **2**, 485 (2013).

[40] R.A. Riggleman, G. Toepperwein, G.J. Papakonstantopoulos, J.L. Barrat, and J.J. De Pablo, J. Chem. Phys. **130**, 244903 (2009).

[41] Y. Li, M. Kröger, and W.K. Liu, Phys. Rev. Lett. **109**, 118001 (2012).

[42] H. Guo, G. Bourret, R.B. Lennox, M. Sutton, J.L. Harden, and R.L. Leheny, Phys. Rev. Lett. **109**, 55901 (2012).

[43] S. Jain, J.G.P. Goossens, G.W.M. Peters, M. van Duin, and P.J. Lemstra, Soft Matter **4**, 1848 (2008).

Curriculum Vitae

Personal Information:

Name:	Michael Langeloth
Birthday:	11th. February 1985
Place of Birth:	Frankfurt am Main, Germany
Nationality:	German

Education:

Jul. 2012	Chemistry (PhD), TU Darmstadt.
Oct. 2005 - Jun. 2012	Chemistry (Diploma), TU Darmstadt.
Jun. 2004	Ricarda-Huch Schule.

Dreieich, den 23. April 2015

Michael Langeloth

Dipl.-Ing. Michael Langeloth
Schiessgartenstrasse 24

63303 Dreieich

Erklärung

Ich erkläre hiermit, noch keinen Promotionsversuch unternommen zu haben.

Dreieich, den 23. April 2015

Michael Langeloth

Dipl.-Ing. Michael Langeloth
Schiessgartenstrasse 24

63303 Dreieich

Erklärung

Ich erkläre hiermit, dass ich meine Dissertation selbständig und nur mit den angegebenen Hilfsmitteln angefertigt habe.

Dreieich, den 23. April 2015

Michael Langeloth